Mathematical Medicine and Biology: A Journal of the IMA (2018) **00**, 1–27
doi:10.1093/imammb/dqy010

Modeling dynamics for oncogenesis encompassing mutations and genetic instability

ARTUR C. FASSONI*
Instituto de Matemática e Computação, UNIFEI, Itajubá, Minas Gerais, Brazil
*Corresponding author. Email: fassoni@unifei.edu.br

AND

HYUN M. YANG
Instituto de Matemática, Estatística e Computação Científica, UNICAMP, Campinas, São Paulo, Brazil

[Received on 17 December 2016; revised on 31 May 2018; accepted on 8 June 2018]

Tumorigenesis has been described as a multistep process, where each step is associated with a genetic alteration, in the direction to progressively transform a normal cell and its descendants into a malignant tumour. Into this work, we propose a mathematical model for cancer onset and development, considering three populations: normal, premalignant and cancer cells. The model takes into account three hallmarks of cancer: self-sufficiency on growth signals, insensibility to anti-growth signals and evading apoptosis. By using a nonlinear expression to describe the mutation from premalignant to cancer cells, the model includes genetic instability as an enabling characteristic of tumour progression. Mathematical analysis was performed in detail. Results indicate that apoptosis and tissue repair system are the first barriers against tumour progression. One of these mechanisms must be corrupted for cancer to develop from a single mutant cell. The results also show that the presence of aggressive cancer cells opens way to survival of less adapted premalignant cells. Numerical simulations were performed with parameter values based on experimental data of breast cancer, and the necessary time taken for cancer to reach a detectable size from a single mutant cell was estimated with respect to some parameters. We find that the rates of apoptosis and mutations have a large influence on the pace of tumour progression and on the time it takes to become clinically detectable.

Keywords: multi-step tumorigenesis; avascular tumour growth; stability; bifurcations.

1. Introduction

Cancer is a complex disease that has more than a hundred different types and can occur in almost all tissues in the body. Although each type of cancer has unique characteristics, the mechanisms that lead to its development are similar and share a few cellular and molecular characteristics. In this way, one can say that almost all cancer types obey certain universal rules (Hanahan & Weinberg, 2000, 2011).

Cancer begins when a mutation occurs in a cell and causes it to escape one of the mechanisms that regulate the process of growth, division and death. However, a single mutation is not enough to develop a malignant tumour, since a diversity of mechanisms exist to preserve tissue integrity. It is necessary that, over the generations, the descendants of the mutant cell accumulate other specific mutations that allow them to surpass the various barriers imposed by the organism against uncontrolled growth. Thus, tumorigenesis is a multistep process, where each step is associated with a genetic change, in the direction of progressive transformation of a normal cell and its descendants into a malignant tumour

(Hanahan & Weinberg, 2000, 2011). Some clinical analyses revealed lesions that would be cells in intermediary stages during the process of cancer formation (Foulds, 1954). Other experiments proved that all cells in a tumour descend from only one common ancestral blackcell (Nowell, 1976). For a detailed description of the biology of cancer, we refer to the book by Weinberg (2013).

Hanahan & Weinberg (2000, 2011) proposed that these genetic and phenotypic alterations can be grouped and conceptually described in eight acquired capabilities, which were denominated the *Hallmarks of Cancer*. They are *self-sufficiency in growth signals*, *insensitivity to anti-growth signals*, *evading apoptosis*, *limitless replicative potential*, *sustained angiogenesis*, *tissue invasion and metastasis*, *reprogramming energy metabolism* and *evading immune destruction*. They also included two *enabling characteristics*, which represent the means that enable populations of premalignant cells to reach the above hallmarks: *genetic instability* and *tumour-promoting inflammation*.

Several works developed mathematical models for carcinogenesis and cancer evolution through multiple stages and using different approaches,such as Ordinary Differential Equations (ODEs) (Spencer *et al.*, 2004; Ashkenazi *et al.*, 2008; Stiehl & Marciniak-Czochra, 2012; Gentry & Jackson, 2013), Partial Differential Equations (PDEs) (Enderling *et al.*, 2007; Bellomo & Delitala, 2008; Marciniak-Czochra & Kimmel, 2008), discrete (Tomlinson & Bodmer, 1995; d'Onofrio & Tomlinson, 2007) and computational models (Abbott *et al.*, 2006; Spencer *et al.*, 2006; Fumiã & Martins, 2013). From the modelling standpoint, our model is more similar to those in Spencer *et al.* (2004); Ashkenazi *et al.* (2008); Gentry & Jackson (2013), and Enderling *et al.* (2007) which consider each hallmark acquisition as a transition between cell populations. Spencer *et al.* (2004) developed an ODE model to analyse how the interplay among angiogenesis, apoptosis, genetic instability and abnormal growth gives rise to different kinetics in tumour progression. Through numerical simulations based on data of breast cancer, they identified particular ordering of such mutations under which cancer develops faster. The group of Gentry developed ODE models that describe the acquisition of hallmarks and included tissue hierarchy, by considering three cell types: stem, progenitor and mature cells (Ashkenazi *et al.*, 2008; Gentry & Jackson, 2013). The model of Enderling *et al.* (2007) considered the development of breast cancer as a step-wise process that involves the loss of function of two tumour suppressor genes by breast stem cells. They also included spatial dynamics (random motion and haptotaxis) for cancer cells. The model predicted that genetic instability and a high number of breast stem cells blackare necessary conditions in order that a tumour arises within a clinically observable time, i.e. within 30 years after puberty.

Here, we present an ODE model to describe the onset of cancer at an initial, avascular stage, with the following hallmarks: *self-sufficiency in growth signals*, *insensitivity to anti-growth signals* and *evading apoptosis*. We also consider the enabling characteristic *genetic instability*. Although the previous models considered more hallmarks or included more complexity, their analysis consisted mostly of numerical simulations. We follow a complementary approach, i.e. a rigourous analysis of a smaller model, which may provide a more mechanistic understanding about the role of each model component. With this, we expect to draw conclusions on how each hallmark acquisition and genetic instability contribute to the process of oncogenesis. At the same time, our theoretical analysis also provides directions to numerical simulations, which we perform blackusing experimental data from the literature to compare our model predictions with clinical observations. Finally, a new feature of our model is the way the mutations are described. While the previous models considered linear transitions, here, based on the interplay between genetic instability and tumour progression, we adopt different mutation terms such as a single-cell transition and a nonlinear term describing a threshold for genetic instability. These assumptions lead to a richer dynamical behaviour which may translate into interesting consequences from the biological point of view.

The paper is organized as follows. Section 2 deals with the development of a mathematical model. In Section 3 we present the mathematical analysis of the model. In Section 4, we obtain parameter values based on literature data. In Section 5, we present numerical simulations and discuss the biological implications of analytical and numerical results. In Section 6, the conclusions are presented.

2. A model for oncogenesis encompassing mutations and genetic instability

We consider the following three cell populations: the *normal* cells at a tissue in the human body are denoted by N; the population of pre-cancer cells with a first hallmark of self-sufficiency in *growth* signals is denoted by G and the population of cancer cells, with both the hallmarks self-sufficiency in growth signals and evading *apoptosis*, is denoted by A. Due to the similarity between the hallmarks of self-sufficiency in growth signals and insensitivity to anti-growth signals, we consider both as a single characteristic acquired by pre-cancer and cancer cells. The model equations are

$$\frac{\mathrm{d}N}{\mathrm{d}t} = r_N - \mu_N N - \beta_1 NA - \beta_4 NG - G_0\delta_D(t-t_0), \tag{2.1a}$$

$$\frac{\mathrm{d}G}{\mathrm{d}t} = r_G G\left(1-\frac{G}{K_G}\right) - (\mu_G+\varepsilon_G)G - \beta_2 NG - \beta_5 AG + G_0\delta_D(t-t_0) - \frac{\delta G^2}{\xi+G}, \tag{2.1b}$$

$$\frac{\mathrm{d}A}{\mathrm{d}t} = r_A A\left(1-\frac{A}{K_A}\right) - (\mu_A+\varepsilon_A)A - \beta_3 NA - \beta_6 AG + \frac{\delta G^2}{\xi+G}. \tag{2.1c}$$

In the following, we briefly present the hypothesis behind model (2.1a). A short description of each parameter is presented in Table 1 (Section 4). Other details can be found in Fassoni & Yang (2016), where we studied a version considering only normal and cancer cells blackwhile including chemotherapy. In that work, our focus was to propose a view on cancer treatment from the ecological resilience perspective.

We assume that the production of normal cells is an intrinsic property of the tissue and adopt a constant production term, described by r_N, and a natural death rate μ_N. On the other hand, due to the self-sufficiency in growth signals, the growth program of pre-cancer and cancer cells is independent of tissue signalling. However, it still depends on nutrient limitation. Thus, a logistic growth is considered, with growth rates r_G and r_A, and carrying capacities K_G and K_A. Parameters μ_G and μ_A are the natural mortality rates of pre-cancer and cancer cells, and ε_G and ε_A are extra mortality rates due to apoptosis (Danial & Korsmeyer, 2004). As cancer cells evaded apoptosis, ε_A is thought to be less than ε_G and can be zero.

Parameters β_i, with $i = 1,\ldots,6$, represent the interactions between cell populations. While in general these terms represent interspecific competition by space and nutrients, here they also comprise other interactions. Parameters β_2 and β_3 embrace the response of the tissue repair system, activated by normal cells in the presence of abnormal cells (Finn, 2008). Parameters β_1 and β_4 describe the damage imposed to normal cells by changes in the local micro-environment introduced by mutant cells, such as increasing the local acidity due to abnormal metabolism (Gatenby & Gawlinski, 2003). Parameters β_5 and β_6 describe the negative effects caused by population G on A, and vice-versa.

We now consider the transitions between cell compartments. In most mathematical models in this context, they are modelled by linear terms like pN or qG, where p and q represent the probabilities of occurrence of mutations/activation of oncogenes, per cell per division (Spencer *et al.*, 2004; Enderling *et al.*, 2007; Gentry & Jackson, 2013). These probabilities are of order of 10^{-8} to 10^{-6} (Tomlinson *et al.*, 1996; Jackson & Loeb, 1998), but not always constant (Loeb, 1991; Negrini *et al.*, 2010; Salk *et al.*, 2010). Indeed, as tumour growth proceeds, the genomes of tumour cells often become increasingly

TABLE 1 *Basic values of parameters adopted in simulations. The values for normal and cancer cells were taken from Fassoni & Yang (2016) and are based on breast cancer. The values for pre-cancer cells were obtained by biological reasoning and comparison with those for cancer cells (see Section 4).*

Parameter	Description	Value
r_N	total constant reproduction of normal cells	10^6 cell day^{-1}
μ_N	$1/\mu_N$ is the lifetime of a normal cell	0.01 day^{-1}
β_1	cancer cells aggressiveness	0.35×10^{-9} cell^{-1}day^{-1}
r_A	cancer cells growth rate	0.05 day^{-1}
K_A	cancer cells carrying capacity	10^8 cells
μ_A	natural mortality rate of cancer cells	0.01 day^{-1}
ε_A	extra mortality rate of cancer cells	0.006 day^{-1}
β_3^{II}	tissue response to cancer cells - case II	0.35×10^{-9} cell^{-1}day^{-1}
r_G	pre-cancer cells growth rate	0.05 day^{-1}
μ_G	natural mortality rate of pre-cancer cells	0.01 day^{-1}
ε_G	extra mortality rate of cancer cells	0.01 day^{-1}
β_2	tissue response to pre-cancer cells	0.35×10^{-9} cell^{-1}day^{-1}
δ	maximal mutation rate of pre-cancer cells	10^{-5} day^{-1}
ξ	threshold for genetic instability	10^3 cells
G_0	initial number of pre-cancer cells	1 cell

unstable, and the rate at which mutations are acquired during each cell generation increases and may exceed the rate at which Darwinian selection can eliminate the less-fit sub-clones of cells (see Sec. 11.7 and Chap. 12 of Weinberg (2013)). Thus, a linear probability rate oversimplifies the reality of cancer and does not capture this departure from the genome's highly stable state when a tumour proceeds Weinberg, 2013 (Loeb, 1991; Negrini *et al*., 2010; Salk *et al*., 2010; Weinberg, 2013).

In our model, we implemented a step-wise process to vary the mutation rate depending on the stage of the tumour development. The first successful transition of a normal cell to a mutant cell is probabilistic (Weinberg, 2013, Chap. 11). Once this viable transition occurs, due to its accelerated growth, the first pre-cancer cell proliferates quickly and acts as a spark to activate cancer. We are interested in analysing whether or not its progeny will be able to survive long enough to reach the next transition stage. As the initial proliferation of these cells is high, the entering of other normal cells in this pool can be neglected. Thus, we model the first effective transition from N to G by a Dirac Delta term, representing that G_0 normal cells became pre-cancerous cells at time t_0 (with the possibility to have $G_0 = 1$),

$$G_0 \delta_D(t - t_0). \tag{2.2}$$

After the onset of pre-cancer cells, their viable mutation is propagated trough cell generations, and there is an increase of genetic instability, so they will be subject to a variable transition from G to A. There is biological evidence that some of the same mutations that increase cell proliferation are also responsible for enhanced genetic instability (Negrini *et al.*, 2010; Salk *et al.*, 2010). In order to include such a threshold effect in the mutation from pre-cancer to cancer cells, we model the transition term as

$$\frac{\delta G^2}{G + \xi}, \tag{2.3}$$

so that the mutation rate $\delta G/(G+\xi)$ is small when there are few cells, increases as the number of cells increases and saturates to the level δ when the number of cells surpasses the threshold defined by ξ. In our model, a linear transition term would be written as δG, with a constant mutation rate δ. Therefore, while previous models considered such linear terms for all transition between cell populations, here, based on the role of genetic instability, the first transition is modelled as a pulse, thereby mimicking a random event, and the second one is a nonlinear flow that approaches a linear one only when a large number of cells is present.

At a first moment, all features of model (2.1a) are important for the context of oncogenesis. However, in order to perform a more detailed analysis, we can disregard some terms which do not have major contribution in the first stage of tumour progression. With this, we obtain a simplified version that still retains the characteristics we want to examine. Since our focus is the appearing of pre-cancer cells, the values of interest are low. Thus, the negative effect caused by them on normal and cancer cells can be neglected, and also the effect suffered by them due to the interaction with cancer cells. Therefore, terms $-\beta_4 NG$, $-\beta_5 AG$ and $-\beta_6 AG$ can be disregarded. By the same reasoning, we disregard the term $-r_G G^2/K_G$. If, in some conclusions we observe that $G \to \infty$, it will be understood that pre-cancer cells reached a stationary state far from $G = 0$, which is what would happen if the logistic term was included. The term $-\beta_2 NG$ in (2.1b) cannot be disregarded because it encompasses the tissue response to pre-cancer cells, which may occur at the very beginning phase. On the other hand, blackcancer cells A constitute the final step in this avascular phase, and all terms in (2.1c) must be kept. By setting the time of first mutation to $t_0 = 0$ and initial conditions $(N(0), G(0), A(0)) = (N_0 - G_0, G_0, 0)$, the model becomes

$$\frac{\mathrm{d}N}{\mathrm{d}t} = r_N - \mu_N N - \beta_1 NA, \tag{2.4a}$$

$$\frac{\mathrm{d}G}{\mathrm{d}t} = r_G G - \beta_2 NG - (\mu_G + \varepsilon_G)G - \frac{\delta G^2}{\xi + G}, \tag{2.4b}$$

$$\frac{\mathrm{d}A}{\mathrm{d}t} = r_A A\left(1 - \frac{A}{K_A}\right) - \beta_3 NA - (\mu_A + \varepsilon_A)A + \frac{\delta G^2}{\xi + G}. \tag{2.4c}$$

3. Model analysis

We now present the mathematical analysis of system (2.4a). We perform an extensive study of the existence and stability of biologically feasible equilibrium points. Biological interpretation and discussion of these results are postponed to Section 5.

3.1 *Trivial equilibrium—Normal cells only*

We start by analysing the trivial equilibrium,

$$P_0 = \left(\frac{r_N}{\mu_N}, 0, 0\right). \tag{3.1}$$

The eigenvalues of the Jacobian matrix of system (2.4a) evaluated at P_0 are

$$\lambda_1^{(0)} = -\mu_N, \quad \lambda_2^{(0)} = \frac{r_N}{\mu_N}(\beta_3^{th} - \beta_3) \quad \text{and} \quad \lambda_3^{(0)} = \frac{r_N}{\mu_N}(\beta_2^{th} - \beta_2), \tag{3.2}$$

where

$$\beta_2^{th} = \frac{\mu_N}{r_N} l_G,\ \beta_3^{th} = \frac{\mu_N}{r_N} l_A,\ \text{with } l_G = r_G - \mu_G - \varepsilon_G,\ \text{and}\ \ l_A = r_A - \mu_A - \varepsilon_A. \tag{3.3}$$

Parameters l_G and l_A can be thought of as the net reproduction rates of cells G and A, respectively, and both will be assumed to be positive. Otherwise, blackpre-cancer cells G and blackcancer cells A would be extinct naturally without interaction with normal cells; see (2.4a). Thus, P_0 is stable if, and only if,

$$\beta_2 > \beta_2^{th} = \frac{l_G}{r_N/\mu_N} \quad \text{and} \quad \beta_3 > \beta_3^{th} = \frac{l_A}{r_N/\mu_N}. \tag{3.4}$$

Therefore, if the negative blackeffects of normal cells on pre-cancer and cancer cells, described by β_2 and β_3, are high, then the tissue is able to eliminate the few mutant cells that arise. If the tissue repair system is not good enough, and one of the two conditions above is not satisfied, P_0 will be unstable, and the blackappearance of a few mutant cells, small disturbances of P_0, will break the tissue homeostatic state free of cancer and will lead to cancer progression with presence of one or two types of mutant cells. Note that larger values of the equilibrium value in the absence of cancer, r_N/μ_N, decrease the thresholds β_i^{th}, and thus increase the protection against cancer. On the other hand, larger values of net reproduction rates l_G and l_A (achieved by evading apoptosis or deregulated growth for instance) increase the thresholds, which increases the risk of cancer onset.

3.2 *Boundary equilibria—absence of pre-cancer cells*

We now analyse the boundary equilibria corresponding to absence of pre-cancer cells. We start presenting previous results about the subsystem formed by equations (2.1a) and (2.1c) with $G = 0$, completely studied in (Fassoni & Yang, 2016, Section 3). These results will be used in the analysis within this section. That subsystem is the restriction of system (2.4a) to the $N \times A$ plane, which is an invariant set of (2.4a). We will refer to this subsystem as subsystem $N \times A$. It has a trivial equilibrium $E_0 = (r_N/\mu_N, 0)$ and two nontrivial equilibria

$$\bar{E}_i = (\bar{N}_i, \bar{A}_i) = \left(\frac{r_N}{\mu_N + \beta_1 \bar{A}_i}, \bar{A}_i \right),\ \ i = 1, 2, \tag{3.5}$$

where $\bar{A}_1$ and $\bar{A}_2$ are the roots of the second-degree polynomial

$$q(A) = aA^2 + bA + c, \tag{3.6}$$

with coefficients

$$a = \beta_1 \frac{r_A}{K_A} > 0, \qquad b = l_A \left(\beta_1^{th} - \beta_1 \right), \qquad c = r_N \left(\beta_3 - \beta_3^{th} \right), \tag{3.7}$$

where

$$\beta_1^{th} = \frac{\mu_N r_A}{l_A K_A}. \tag{3.8}$$

These roots satisfy $\bar{A}_1 < \bar{A}_2$ when both are real. An important threshold to this analysis is given by

$$\beta_{1,\Delta}^{th} = \beta_1^{th} + 2\eta + 2\sqrt{\eta(\beta_1^{th} + \eta)}, \tag{3.9}$$

where $\eta = r_A r_N(\beta_3 - \beta_3^{th})/(K_A l_A^2)$. Notice that it is defined only for $\beta_3 > \beta_3^{th}$.

In Fassoni & Yang (2016), we showed that subsystem $N \times A$ has one of the three behaviours:

I) If $\beta_3 > \beta_3^{th}$ and $\beta_1 < \beta_{1,\Delta}^{th}$: $\bar{A}_1$ and $\bar{A}_2$ either are real and negative or complex conjugate, so that $\bar{E}_1$ and $\bar{E}_2$ are not biologically feasible; E_0 is globally stable.

II) If $\beta_3 > \beta_3^{th}$ and $\beta_1 > \beta_{1,\Delta}^{th}$: $\bar{A}_1$ and $\bar{A}_2$ are real and positive, E_0 and $\bar{E}_2$ are locally stable and $\bar{E}_1$ is a saddle-point.

III) If $\beta_3 < \beta_3^{th}$: the roots satisfy $\bar{A}_1 < 0 < \bar{A}_2$, E_0 is a saddle-point and $\bar{E}_2$ is globally stable for initial conditions with $A(0) > 0$.

By setting $G = 0$ in (2.4a), we see that each equilibrium (N, A) of subsystem $N \times A$ corresponds to one boundary equilibrium (N, G, A) of system (2.4a). Thus, besides the trivial equilibria P_0, system (2.4) has two nontrivial boundary equilibria given by

$$\bar{P}_i = (\bar{N}_i, 0, \bar{A}_i) = \left(\frac{r_N}{\mu_N + \beta_1 \bar{A}_i}, 0, \bar{A}_i\right), \quad i = 1, 2. \tag{3.10}$$

These equilibria have positive coordinates under the conditions II and III stated above.

We now analyse the linear stability of these equilibria. The Jacobian matrix of system (2.4a) evaluated at $\bar{P}_i$ is given by

$$J(\bar{P}_i) = \begin{bmatrix} -\beta_1 \bar{A}_i - \mu_N & 0 & -\beta_1 \bar{N}_i \\ 0 & l_G - \beta_2 \bar{N}_i & 0 \\ -\beta_3 \bar{A}_i & 0 & l_A - 2\frac{r_A}{K_A}\bar{A}_i - \beta_3 \bar{N}_i \end{bmatrix}, \quad i = 1, 2. \tag{3.11}$$

The characteristic polynomial $p(\lambda)$ of $J(\bar{P})$ factors as

$$p(\lambda) = (l_G - \beta_2 \bar{N} - \lambda) p_2(\lambda) \tag{3.12}$$

where $p_2(\lambda)$ is the characteristic polynomial of the Jacobian matrix of subsystem $N \times A$ evaluated at $\bar{E}_i$,

$$j(\bar{E}_i) = \begin{bmatrix} -\beta_1 \bar{A} - \mu_N & -\beta_1 \bar{N} \\ -\beta_3 \bar{A} & l_A - 2\frac{r_A}{K_A}\bar{A} - \beta_3 \bar{N} \end{bmatrix}. \tag{3.13}$$

We know the eigenvalues of $j(\bar{E}_i)$ from the results about stability of $\bar{E}_i$ in subsystem $N \times A$ (conditions II and III above). They are also eigenvalues of $J(\bar{P}_i)$. The third eigenvalue of $J(\bar{P}_i)$ is

$$\lambda_3^{(i)} = l_G - \beta_2 \bar{N}_i = \frac{r_N}{\mu_N + \beta_1 \bar{A}_i}(\beta_{2,\lambda}^{th,i} - \beta_2), \tag{3.14}$$

where

$$\beta_{2,\lambda}^{th,i} = \beta_2^{th} + \frac{l_G \beta_1 \bar{A}_i}{r_N} > \beta_2^{th}, \;\; i = 1, 2. \tag{3.15}$$

Therefore, we conclude that $\bar{P}_1$ will be unstable whenever it is positive (case II above), with one positive eigenvalue if $\beta_2 > \beta_{2,\lambda}^{th,1}$, and two positive eigenvalues otherwise. Regarding the point $\bar{P}_2$, if $\beta_2 > \beta_{2,\lambda}^{th,2}$, it will be stable whenever it is positive (cases II and III above). Otherwise, $\bar{P}_2$ will be unstable, with one positive eigenvalue.

3.3 *Internal equilibria—presence of pre-cancer and cancer cells*

We now analyse the internal equilibria of system (2.4), given by $\tilde{P} = (\tilde{N}, \tilde{G}, \tilde{A})$. Here, $\tilde{N}$ and $\tilde{G}$ are given in terms of $\tilde{A}$,

$$\tilde{N} = \frac{r_N}{(\mu_N + \beta_1 \tilde{A})}, \qquad \tilde{G} = \frac{\xi \left(l_G(\mu_N + \beta_1 \tilde{A}) - \beta_2 r_N \right)}{\beta_2 r_N - (l_G - \delta)(\mu_N + \beta_1 \tilde{A})}, \tag{3.16}$$

and $\tilde{A}$ is a root of the fourth-degree polynomial equation

$$f(A) = g(A), \tag{3.17}$$

with

$$f(A) = \beta_1 (l_G - \delta)\, A\, q(A)\, (A_M - A) \quad \text{and} \quad g(A) = \xi\, l_G^2\, \beta_1^2\, (A - A_m)^2 . \tag{3.18}$$

Here, $q(A)$ is the second-degree polynomial given in (3.6), and A_m and A_M are given by

$$A_m = \frac{r_N}{\beta_1 l_G} \left(\beta_2 - \beta_2^{th} \right), \; A_M = \frac{r_N}{\beta_1 (l_G - \delta)} \left(\beta_2 - \beta_{2,\delta}^{th} \right), \;\; \beta_{2,\delta}^{th} = \frac{\mu_N (l_G - \delta)}{r_N}. \tag{3.19}$$

The fourth-degree polynomial equation (3.17) admits up to four roots. Thus, we have up to four equilibrium points $\tilde{P}_i = (\tilde{N}_i, \tilde{G}_i, \tilde{A}_i)$, $i = 3, 4, 5, 6$. We analysed the existence and positiveness of equilibria $\tilde{P}_i$ in the entire parameter space and the results are summarized in Fig. 1. The proof of these results and additional details are given in Appendix A.

Stability analysis of equilibria $\tilde{P}_i$, $i = 3, 4, 5, 6$, is done by studying the roots of the characteristic equation of the jacobian matrix of (2.4) evaluated at $\tilde{P}_i$. The characteristic equation is

$$\lambda^3 + a_1 \lambda^2 + a_2 \lambda + a_3 = 0, \tag{3.20}$$

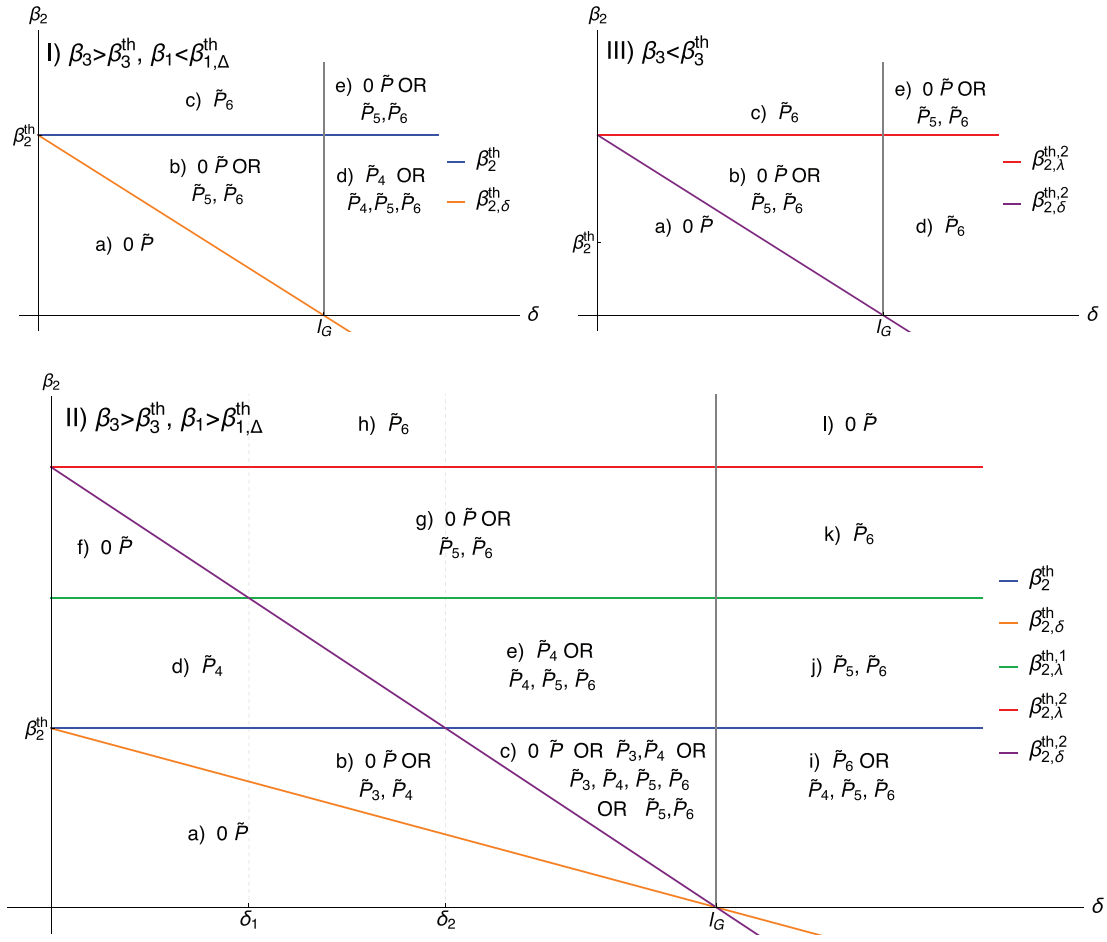

FIG. 1. Existence of positive internal equilibria $\tilde{P}_i$, $i = 3,4,5,6$, depending on β_2 and δ. On the top left, we have the case I) $\beta_3 > \beta_3^{th}$ and $\beta_1 < \beta_{1,\Delta}^{th}$; on the top right, the case III) $\beta_3 < \beta_3^{th}$; at the bottom, the case II) $\beta_3 > \beta_3^{th}$ and $\beta_1 > \beta_{1,\Delta}^{th}$. In each case, the parameter sub-regions are separated by the thresholds indicated in the legend. At those regions where there is the word 'OR', the existence of some internal equilibria also depends on other conditions. Details are presented in Appendix A.

with coefficients

$$
\begin{aligned}
a_1 &= \beta_1\tilde{A} + \mu_N + \frac{\xi(l_G - \beta_2\tilde{N})}{\tilde{G}+\xi} - d,\\
a_2 &= -d\left(\frac{\xi(l_G - \beta_2\tilde{N})}{\tilde{G}+\xi} + \beta_1\tilde{A} + \mu_N\right) + \frac{\xi(l_G - \beta_2\tilde{N})}{\tilde{G}+\xi}\left(\beta_1\tilde{A} + \mu_N\right) - \beta_1\beta_3\tilde{N}\tilde{A},\\
a_3 &= -d\frac{\xi(l_G - \beta_2\tilde{N})}{\tilde{G}+\xi}\left(\beta_1\tilde{A} + \mu_N\right) - \beta_1\tilde{N}\frac{(l_G - \beta_2\tilde{N})}{\tilde{G}+\xi}\left(\beta_2\tilde{G}(\tilde{G}+2\xi) - \beta_3\tilde{A}\xi\right),
\end{aligned}
\tag{3.21}
$$

where $\tilde{N}$, $\tilde{G}$ are given in (3.16), $\tilde{A}$ is a root of (3.17) and $d = (l_A - 2\frac{r_A}{K_A}\tilde{A} - \beta_3\tilde{N})$. According to the Routh–Hurwitz criteria, an equilibrium $\tilde{P}$ is stable if

$$a_1 > 0, \quad a_3 > 0 \quad \text{and} \quad a_1a_2 - a_3 > 0. \tag{3.22}$$

We studied these conditions by combining the analytical results on the existence of positive equilibria $\tilde{P}_i$ with numerical bifurcation analysis using the software *Mathematica*©. With this, we analysed the stability of equilibria $\tilde{P}_i$ in all regions of the parameter space. Figure 2 presents a sketch of the parameter space and indicates which are the stable equilibria in each sub-region of the parameter space. Figure 3 summarizes all results about the existence and stability of the equilibria of system (2.4). The complete details and explanations about the methods we used are given in Appendix A.2.

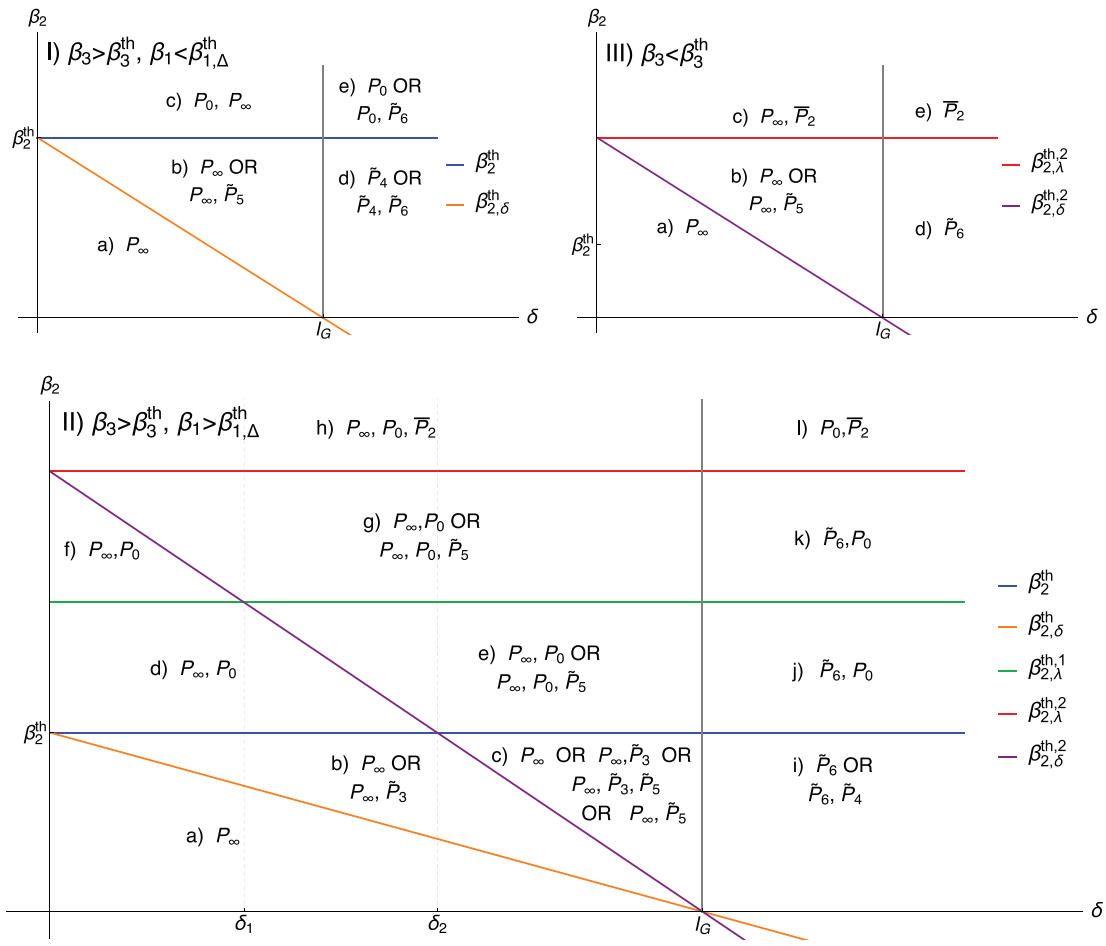

FIG. 2. This figure shows which equilibria are locally stable in each sub-region of parameter space. At regions where there is the word 'OR', the existence of some internal equilibria also depends on other conditions. These results were obtained by combining analytical and numerical results, as detailed in Appendix A.

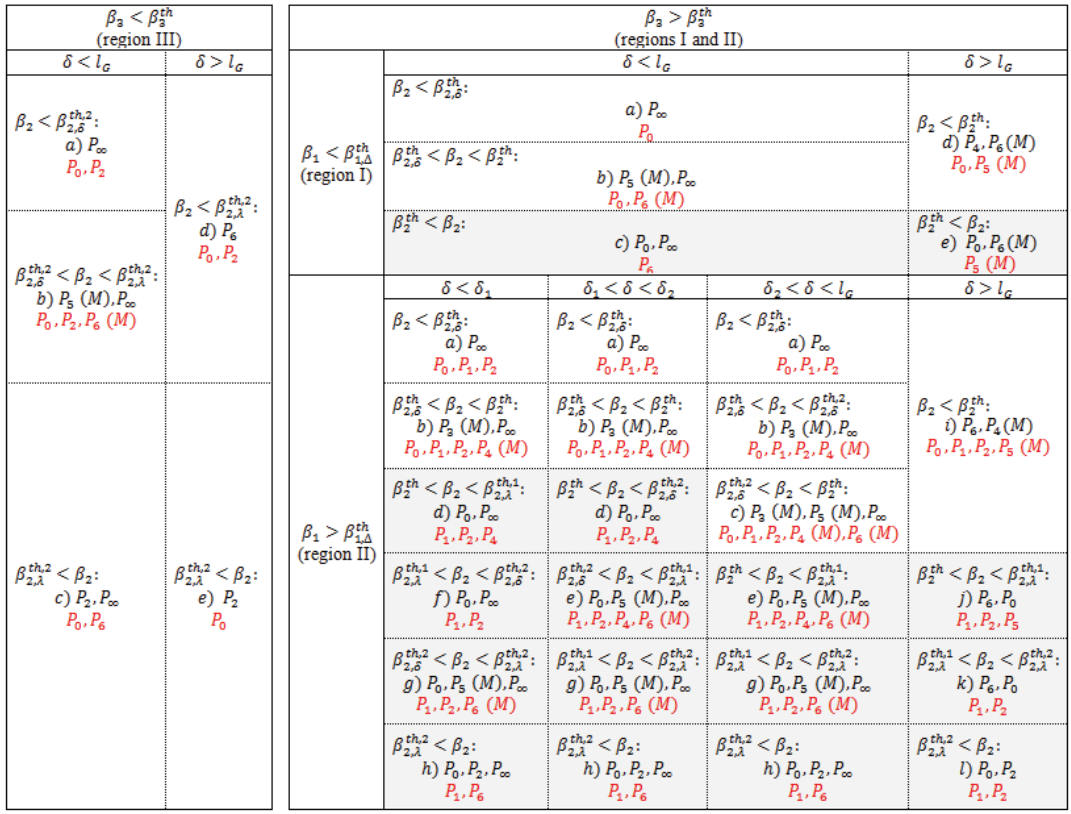

FIG. 3. This scheme shows which equilibrium points are positive in each range of parameters space. In each region where '(M)' appears after two points, a collision between these two points can occur depending on other parameters, and the points can be both positive or not. Stability of equilibria is also indicated: black for stable, and red for unstable. Highlighted cells represent ranges of parameter space where P_0 is stable, i.e. cancer can be eliminated. All results for points P_0, $\tilde{P}_1$ and $\tilde{P}_2$, and those about positiveness of points $\tilde{P}_i$, $i = 3, 4, 5, 6$, were mathematically proved, while results about stability of $\tilde{P}_i$, $i = 3, 4, 5, 6$ and P_∞ were obtained numerically. See Appendix A for details.

In order to illustrate these analytical and numerical results on existence and stability of internal equilibria, we obtained phase portraits corresponding to each region in Figs 2 and 3. It was done by solving system (2.4) numerically with *Mathematica*©, with an implicit Runge–Kutta method. Some of these phase portraits are presented in Fig. 4, while the others are not shown for sake of brevity. In all cases shown in Fig. 4 it can be seen that some solutions (red trajectories) approach a point at 'infinity' such as $(N, G, A) = (N, \infty, \infty)$. This point will be denoted by P_∞. As commented in Section 2, P_∞ represents the survival of G cells at a quantity very far from $G = 0$, due to the lack of a logistic term in the dynamics of G. We also see in Figs 2 and 3 that there are subsets of the parameter space where the phase space is divided into three basins of attraction, as illustrated by phase portraits II)e) and II)h) in Fig. 4. Therefore, the model outcomes are highly dependent not only on the parameters regimens, but also on the initial conditions.

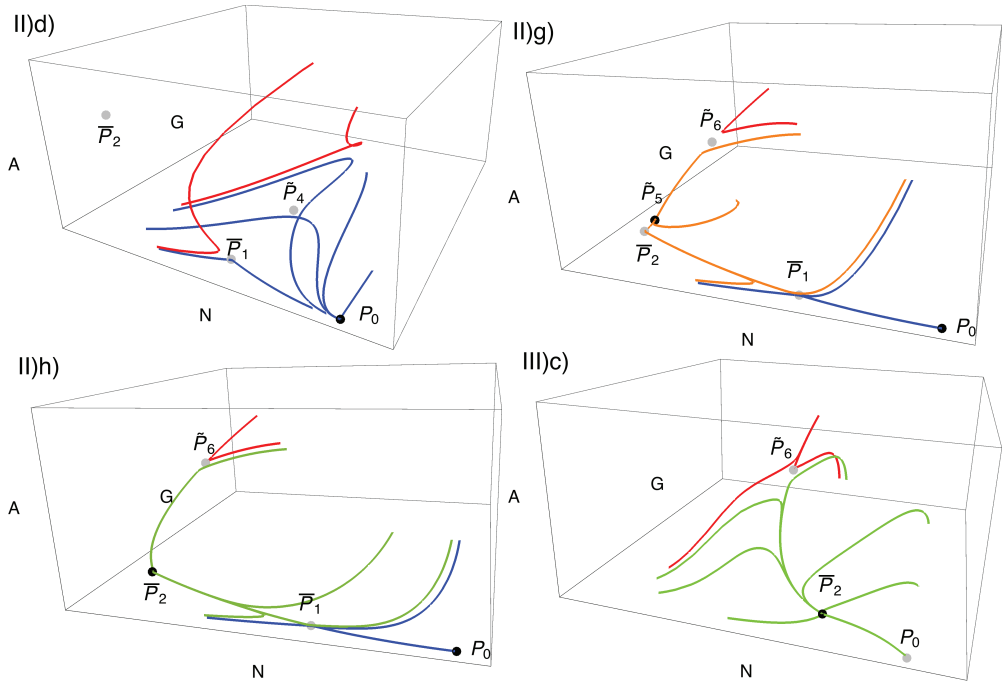

FIG. 4. Phase portraits of system (2.4) for parameter values corresponding to some cases of Fig. 3. Stable equilibrium points are indicated by black dots, while saddle or unstable equilibrium points are indicated by grey dots. The trajectories are coloured according to the equilibrium they converge to: P_0 (blue, normal cells only), $\tilde{P}_2$ (green, no pre-cancer cells), $\tilde{P}_5$ (orange, all cell types) and P_∞ (red, all cell types, with $G, A \to \infty$). Case II)d): phase space is divided in the basins of attraction of P_0 and P_∞. Region II)g): phase space is divided in the basins of attraction of P_0, $\tilde{P}_5$ and P_∞. Case II)h): phase space is divided in the basins of attraction of P_0, $\tilde{P}_2$ and P_∞. Case III)c): phase space is divided in the basins of attraction of $\tilde{P}_2$ and P_∞.

4. Model parametrization

In this section we obtain values for parameters in order to illustrate the discussions with clinical relevant simulations and to assess how some key parameters influence on the quantitative behaviour of the model. The basic values for parameters of normal and cancer cells were taken from Fassoni & Yang (2016), where we obtained values relevant for breast cancer Spencer *et al.* (2004). These parameters are presented in Table 1. We now present the values for pre-cancer cells.

- Using the same value of r_A set in Fassoni & Yang (2016), we assume that the growth rates of pre-cancer and cancer cells are the same, $r_G = r_A = 0.05$ days^{-1}. Since cancer cells have evaded apoptosis while blackpre-cancer cells do not, and $\varepsilon_A = 0.01$ days^{-1} is used in Fassoni & Yang (2016), we assume $\varepsilon_G = 0.01$ days^{-1}, and values for ε_A in the range $0 \leqslant \varepsilon_A \leqslant 0.01$.
- Concerning mutation rates, in the literature, the probability of a mutation occurring in a gene during cell division is estimated to be from 10^{-8} to 10^{-6} (Tomlinson *et al.*, 1996; Jackson & Loeb, 1998). Also, it is assumed that approximately 100 genes are involved in a same physiological change that characterizes a hallmark of cancer, like evading apoptosis or self-sufficiency in growth signals (Spencer *et al.*, 2004). Thus, we consider the gene mutation

probability to be 10^{-7} and multiply it by 100 in order to obtain the maximal mutation rate $\delta = 10^{-5}$. The threshold of genetic instability, at which the effective mutation rate reaches half the value of δ, was initially set to $G = \xi = 10^3$ cells.

- The values of interacting parameters β_1, β_2 and β_3, in units of cell^{-1}day^{-1}, are unknown *a priori* but, by substituting the values of other parameters, it is possible to obtain at least the values for the thresholds to β_1, β_2 and β_3. Using the previous parameter values, and $\varepsilon_A = 0.01$ day^{-1}, the thresholds are given by $\beta_2^{th} = \beta_3^{th} = 0.30 \times 10^{-9}$, $\beta_1^{th} = 0.17 \times 10^{-9}$ and $\beta_{1,\Delta}^{th} = 0.37 \times 10^{-9}$. As we want to observe the different behaviours when β_i, $i = 1, 2, 3$, are greater or lesser than these thresholds, we start with the following basic values for them, $\beta_1 = \beta_2 = \beta_3 = 0.35 \times 10^{-9}$ cell^{-1}day^{-1}, which corresponds to Region I) c) of parameter space (see Figs 2 and 3).

5. Discussion

We now turn to discuss the biological implications of qualitative analysis in Section 3. We illustrate the discussion with numerical simulations. Here, we omit the units of the parameters (see Table 1).

5.1 *Cancer onset from very few cells*

First, we analyse the results from the point of view of cancer onset from very few mutant cells. We focus our attention to specific regions of parameters space where tumour progression is possible from very few cells. Thus, we must consider regions where P_0 is not stable, because the more biologically relevant initial conditions in this viewpoint are small disturbances from P_0, and these solutions would return to P_0 if blackthis equilibrium is stable.

If we disregard the mutation from G to A for a moment ($\delta = 0$), we have the following. When $\beta_2 < \beta_2^{th}$, normal cells fail to prevent the growth of G cells, because $G \to \infty$ (see (2.4) and (3.3)). In this case, there is no need for G cells to acquire a second hallmark. On the other hand, if $\beta_2 > \beta_2^{th}$, normal cells are capable of preventing the growth of G cells, and $G \to 0$. In this case, the hallmark of self-sufficiency in growth signals is not enough for the development of these mutant cells, and it is necessary that these cells acquire another hallmark that increases their survival chances. Thus, if we require that the mutation from G to A is a necessary step, then, the more biologically plausible regions are those where $\beta_2 > \beta_2^{th}$. Following these conditions, we observe that in regions I and II, when $\beta_3 > \beta_3^{th}$, there is no chance for cancer onset from very few mutant cells, since in all sub-regions, P_0 is locally stable if $\beta_2 > \beta_2^{th}$. Therefore, cancer onset from very few mutant cells is possible only in region III, with $\beta_3 < \beta_3^{th}$. Thus, the mutation from G cells to A cells represents the condition of mutant cells adapting, which requires mutation from a population with $\beta_2 > \beta_2^{th}$ to one which satisfies $\beta_3 < \beta_3^{th}$. Next we examine this condition in more detail.

5.2 *Evading apoptosis and decreasing tissue response against cancer are necessary conditions for cancer onset from very few cells*

The condition for cancer onset from very few cells, $\beta_3 < \beta_3^{th}$, is equivalent to

$$\beta_3 + \frac{r_N}{\mu_N}\varepsilon_A < \frac{r_N}{\mu_N}(r_A - \mu_A). \tag{5.1}$$

This condition will be satisfied if the apoptosis rate of cancer cells is reduced (low ε_A) and/or if the repair system is not strong enough (low β_3). Under these conditions, the tissue is not able to prevent tumour growth and the appearance of a few mutant cells will break the homeostatic state in the tissue and lead to a tumour with the presence of one or two types of mutant cells. Thus, the first barrier to tumour progression is broken by evading apoptosis and/or the disruption of the repair system against cancer cells. With respect to evading apoptosis, it is well known as one of the major hallmarks of cancer (Hanahan & Weinberg, 2011). With respect to disruption of repair systems, these conclusions agree with the evidences that the probability of tumour progression is often enhanced in injured organs and tissues that display lost or diminished regenerative ability (Ruggiero & Bustuoabad, 2006).

Even if condition (5.1) is satisfied, apoptosis and tissue response can also be barriers to tumour progression from a quantitative point of view. We illustrate this by numerical simulations, assuming parameter values in Table 1 and assessing the outcome of varying ε_A and β_3. We suppose that a single pre-cancer cell arises at time $t = 0$, i.e. $G_0 = 1$. Initially, we consider that the apoptotic rate of cancer cells is 40% less than the rate of pre-cancer cells, $\varepsilon_A = 0.006$. With these parameters values we have the threshold $\beta_3^{th} = 0.34 \times 10^{-9}$. If we consider that the tissue responses to pre-cancer and cancer cells are the same, $\beta_3 = 0.35 \times 10^{-9} > \beta_3^{th}$, then we are in region I) c) of parameters space, where P_0 is locally stable. Figure 5 (A) shows the corresponding simulation, and we see that pre-cancer and cancer cells are eliminated. In order to have the possibility of cancer progression, the condition $\beta_3 < \beta_3^{th}$ must be satisfied. This can be expressed for parameter ε_A: if we set $\beta_3 = 0.35 \times 10^{-9}$, the condition becomes $\varepsilon_A < 0.005$. Therefore, in the next simulation we decrease the apoptosis rate of cancer cells by half, to $\varepsilon_A = 0.003$ (Fig. 5 (B)). With this value, we pass to region III, where P_0 is unstable and cancer onset is possible from a qualitative point of view. However, the simulation indicates that cancer cells take 42 years to reach the stationary population of 0.52×10^6 cells. Based on Schabel (1975), we assume that cancer is detectable when it attains a tumour with 10^6 cells. Thus, in this simulation the final tumour is clinically undetectable. Therefore, even if the cancer can develop from a qualitative point of view (the apoptosis rate is small so that P_0 is unstable), it can take too long to reach the final size, which is still undetectable. Thus, a quantitative decrease of the apoptosis rate is necessary to reach a detectable size during a human lifetime. This is illustrated in panel (C). In this simulation, assuming that cancer cells have completely evaded apoptosis, $\varepsilon_A = 0$, the cancer takes only 18 years to reach the equilibrium population with 1.3×10^6 cells, which now is detectable. Evasion of tissue response by cancer cells also accelerates tumour progression and increases its final size. As an example, Fig. 5 (D) shows a simulation where cancer cells have completely evaded apoptosis ($\varepsilon_A = 0$), and the tissue response to cancer cells decreased by 20%, $\beta_3 = 0.28 \times 10^{-9}$. With these values, the tumour reaches an equilibrium size with 2.9×10^6 cells within 8 years. A summary of these simulations is given in Table 2.

TABLE 2 *Effects of parameter changes on the final tumour size (S, number of cancer cells) and the time needed to reach final size (T, in years). With exception of the parameters varied in each simulation (row), all other parameter values are those of Table 1.*

Values	Size S	Time T	Detectable	Figure
$\varepsilon_A = 0.006, \beta_3 = 0.35 \times 10^{-9}$	0	-	no	5 (A)
$\varepsilon_A = 0.003, \beta_3 = 0.35 \times 10^{-9}$	0.52×10^6	42y	no	5 (B)
$\varepsilon_A = 0, \beta_3 = 0.35 \times 10^{-9}$	1.3×10^6	18y	yes	5 (C)
$\varepsilon_A = 0, \beta_3 = 0.28 \times 10^{-9}$	2.9×10^6	8y	yes	5 (D)

We analyse in more detail how β_3 and ε_A modify the necessary time for cancer to attain a clinically detectable size. Simulations of system (2.4), with initial condition $G_0 = 1$, and different values of ε_A and β_3, were performed. In each simulation, we seek the first time at which cancer cells (either A or G) reached the detectable size of 10^6 cells. Results are shown in Fig. 6. We see that diminishing both the tissue response and tumour intrinsic apoptotic rate blackleads to a smaller time for tumour development, which can vary from larger values, e.g. 21 years, to small ones, e.g. 2 years. Thus, besides predicting qualitatively that evading apoptosis allows cancer development, the model also agrees quantitatively with biological facts by showing that evading apoptosis increases the velocity of tumour progression. It is also worth noting that there are intervals of parameters β_3 and ε_A for which the tumour attains a maximum size smaller than the clinically detectable size. So the model also predicts the onset and establishment of cancer at non-detectable, avascular stage, but which may suffer other mutations that enable other hallmarks, such as angiogenesis and subsequent invasion and metastasis.

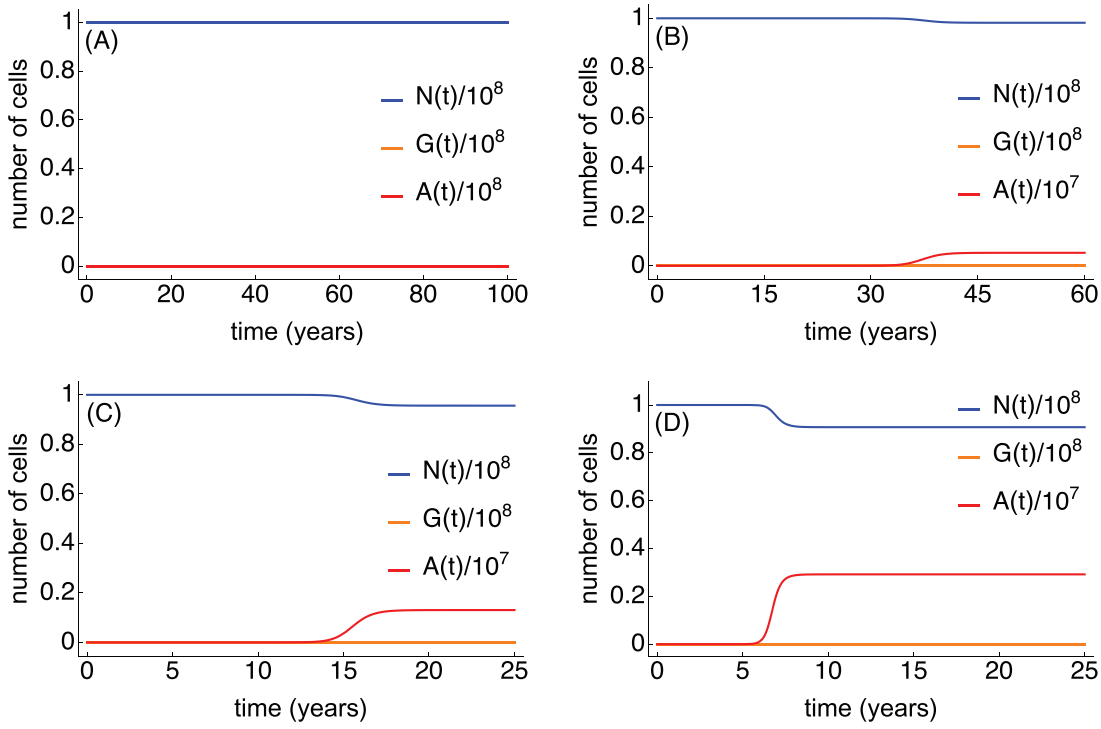

FIG. 5. Simulations of system (2.4) with initial condition $G_0 = 1$. In the first simulation, with parameter values given in Table 1, cancer cells are eliminated (A). If cancer cells partially evade apoptosis ($\varepsilon_A = 0.003$), then they are able to survive, but it takes 42 years to reach the undetectable size of 0.52×10^6 cells (B). If cancer cells completely evade apoptosis ($\varepsilon_A = 0$), it takes 18 years to reach the detectable size of 1.3×10^6 cells (C). Finally, panel (D) shows the effect of evading apoptosis ($\varepsilon_A = 0$) combined with a decreasing in the tissue response by 20%, $\beta_3 = 0.28 \times 10^{-9}$. In this case, cancer cells reach the stationary size of 2.2×10^6 cells in only 4 years.

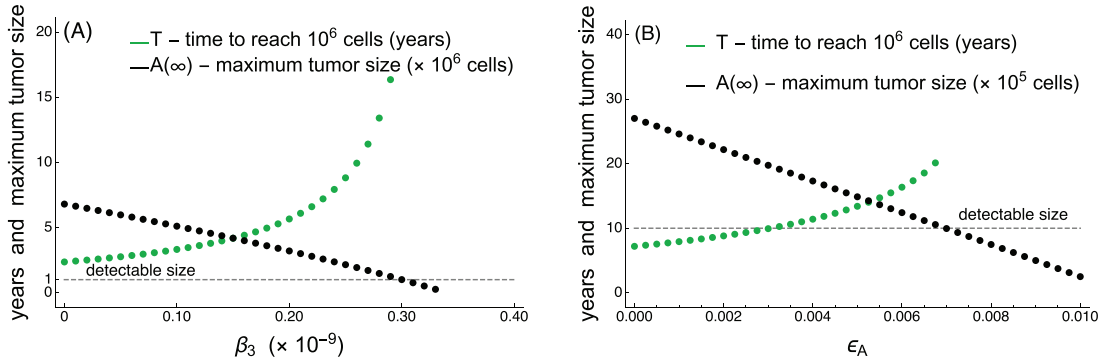

FIG. 6. Necessary time for cancer to reach detectable size (10^6 cells), beginning with a single mutant pre-cancer cell black $G_0 = 1$. (A) The effect of varying β_3 is shown (with $\varepsilon_A = 0.006$ fixed): for values of β_3 near zero, cancer attains detectable size in only 2.5 years; as the tissue response is increased, this time grows up to 17 years; for $0.29 \times 10^{-9} < \beta_3 < 0.34 \times 10^{-9}$, the maximum tumour size is below detectable size; for $\beta_3 > 0.34 \times 10^{-9} = \beta_3^{th}$, cancer cells are eliminated (P_0 is stable). (B) The effect of varying ε_A is assessed (with $\beta_3 = 0.29 \times 10^{-9}$ fixed): the necessary time to reach a detectable size varies from 7 years to 21 years; for $0.007 < \varepsilon_A < 0.010$, the maximum tumour size is below detectable size; for $\varepsilon_A > 0.010$ (not shown), cancer cells are eliminated (P_0 is stable).

5.3 *Genetic instability is an enabling characteristic for tumour progression*

We now analyse the effect of genetic instability, which may blackalter the values of mutation rate and the initial number of mutant cells. Initially, we assess the role of genetic instability by changing the values of the mutation rate δ and comparing the sub-cases in Region III of parameter space as δ increases (see Fig. 2). In subsystem $N \times A$, we have cancer growth, since $\bar{E}_2$ is globally stable in this subsystem. To understand what happens in the system (2.4), we consider two possibilities: $\delta < l_G$ and $\delta > l_G$. The first one can be rewritten as $\delta + \varepsilon_G < r_G - \mu_G$. Thus, the sum of mutation rate and additional apoptotic rate of G is low, lesser than the net growth rate. In this scenario, blackwe have the following:

Case a: if $\beta_2 < \beta_{2,\delta}^{th,2}$ (which is possible even with $\beta_2 > \beta_2^{th}$—see Fig. 3), P_∞ is globally stable and cancer grows in the tissue achieving a high number of cells. It happens because the presence of tumour cells A resistant to the tissue response leads to a decrease in the quantity of N cells. These cells, in a lesser number, do not blackcreate enough pressure to eliminate G cells. Thus, while at an initial instant pre-cancer cells G work as a trigger to development of cancer cells A, at a subsequent instant, cancer cells A open space in the tissue for the development of less adapted cells, which would not survive in the absence of the more adapted A cells. This feedback leads to a heterogeneous tumour, with distinct cell subpopulations.

Case b: increasing tissue aggressiveness against G cells, if $\beta_{2,\delta}^{th} < \beta_2 < \beta_{2,\lambda}^{th}$, $\tilde{P}_5$ becomes stable. Thus, initial conditions near P_0 will converge to $\tilde{P}_5$. A heterogeneous tumour establishes in the tissue, but attains a steady state level less than the encountered in the previous case.

Case c: increasing the tissue response, $\beta_2 > \beta_{2,\lambda}^{th}$, $\tilde{P}_5$ ceases to exist and $\bar{P}_2$ becomes stable. Thus, initial conditions near P_0 will converge to $\bar{P}_2$. Therefore, in this case, the tissue high aggressiveness against blackpre-cancer cells G does not allow the survival of them, and the final tumour is not heterogeneous as in the previous case. However, the onset of pre-cancer cells works at least as a trigger to tumour progression, since it enables blackcancer cells A, to attain a positive stationary state.

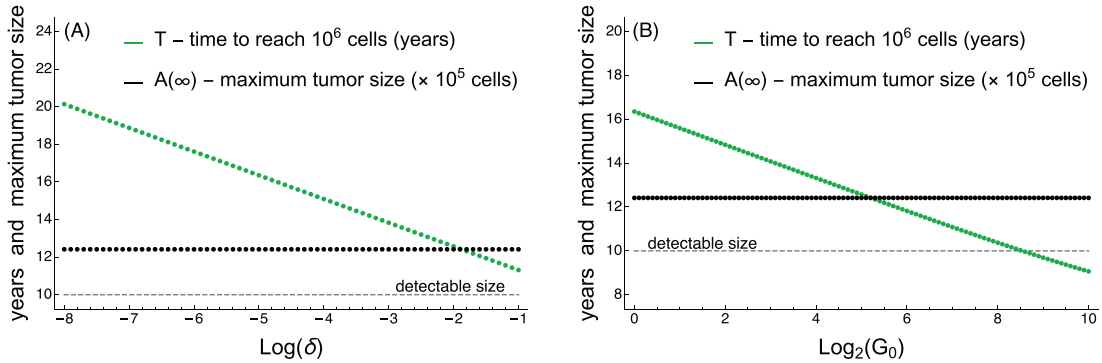

FIG. 7. Necessary time for cancer to reach the detectable size (10^6 cells), beginning with a G_0 mutant cells. (A) The effect of varying δ, with $G_0 = 1$ fixed. (B) The effect of varying G_0, with $\delta = 10^{-5}$ fixed. Parameter values are indicated in the text.

The other possibility, $\delta + \varepsilon_G > r_G - \mu_G$, is similar to the previous case. The difference is that the high apoptotic rate ε_G does not allow blackpre-cancer cells G to attain high levels (P_∞ is not stable).

From a quantitative point of view, the effects of varying δ are shown in Fig. 7 (A). As δ increases, the time T for cancer to reach the detectable size diminishes linearly with $\log \delta$, according with $T = 10.05 - 1.26 \log \delta$. So, a 10 fold increase in the mutation rate diminishes the time T by 1.26 years. At the standard value $\delta = 10^{-5}$ we have $T = 16.3$ years. When $\delta = 10^{-3}$, we have $T = 13.8$ years.

Besides increasing the mutation rate of cells, genetic instability and tissue exposure to carcinogenic factors may blackalso increase the initial number of premalignant cells, described by G_0 in the model. The effect of increasing G_0 is illustrated in the plot of T versus $\log_2 G_0$ in Fig. 7 (right). The parameter values are those in Table 1, with $\beta_3 = 0.29 \times 10^{-9}$, $\varepsilon_A = 0.006$. When $G_0 = 1$, we have $T = 16.3$ years. As G_0 increases, T decreases linearly with $\log_2 G_0$ according to equation $T = 16.3 - 0.74 \log_2 G_0$. Therefore, doubling the initial number of pre-cancer cells leads to a reduction of approximately 9 months in the time taken for the tumour to reach 10^6 cells.

As seen above, specially in Fig. 7, small changes in the mutation rate or the initial number of mutant cells have a large impact on the pace of tumour progression. These results illustrate the fact that the differences between a cancer patient and a healthy person may not be structural or qualitative differences between their intrinsic cellular systems, i.e. differences in parameters that lead to different regions on parameters space, some where P_0 is stable and other where P_0 is unstable. On the contrary, the unique difference between these people could be only quantitative, in the sense that virtually both will have cancer some day, but after different times, due to the differences between the mutation rate or exposure to carcinogenic factors. From this point of view, genetic instability is the major factor that leads to tumour progression within a clinically observable time. These results agree with the understanding that genetic instability is an enabling characteristic of cancer (Hanahan & Weinberg, 2011), and with results of Enderling *et al.* (2007), which predicts that normal mutation rates give rise to a tumour within a human lifetime only if genetic instability is a driving force of the mutation pathway.

5.4 *The feedback effect between cancer and pre-cancer cells*

Finally, we comment on the role of pre-cancer cells and their mutation to cancer cells. We turn attention to region I of parameter space, where cancer cells would be extinct if there would not be pre-cancer cells, since P_0 is globally stable in subsystem $N \times A$. In the full system, we see in Fig. 3 that P_0

is not globally stable anymore. Under the more realistic condition $\beta_2 > \beta_2^{th}$ (where pre-cancer cells would be eliminated if they do not mutate into cancer cells, as discussed above) P_0 is only locally stable. Therefore, under high genome instability which increases initial conditions favourable for pre-cancer and cancer cells, the constant transition from pre-cancer to cancer cells may sustain the tumour progression in scenarios where both of these cell populations could not survive alone.

6. Conclusion

An ordinary differential equation model considering normal, pre-cancer and cancer cells was proposed to describe cancer onset and progression considering three hallmarks of cancer: self-sufficiency on growth signals, insensibility to anti-growth signals and evading apoptosis. Transitions between compartments were modelled differently from previous works, by using Dirac Deltas and a continuous nonlinear flux in order to capture the effects of genetic instability as a factor that enhances the probabilities of mutations. Combining analytical and numerical methods, the model was studied in detail and the existence and stability of steady states were characterized in the entire parameter space, allowing to obtain a global description of model behaviour.

Previous models approaching oncogenesis have been analysed mostly with numerical simulations and the results provided insights on several aspects of tumour progression, mainly with focus on optimal orders of hallmark acquisition which accelerate cancer progression (Spencer *et al.*, 2004; Ashkenazi *et al.*, 2008; Gentry & Jackson, 2013), but also on implications of genetic instability on the pace of tumour progression black (Enderling *et al.*, 2007). Here, the qualitative approach adopted to analyse the model allowed us to study oncogenesis from a more mechanistic point of view.

We showed that pre-malignant cells with self-sufficiency in growth signals cannot survive without a further step to a more malignant phenotype, through evasion of apoptosis or corruption of the tissue repair system. At the same time, the analysis also predicted that the presence of these aggressive cancer cells allows the survival of those less adapted pre-cancer cells which would not survive alone, thereby leading to formation of a heterogeneous tumour. Interestingly, in a scenario where neither the pre-cancer would survive without suffering mutations, nor the cancer cells would persist in the absence of pre-cancer cells, the model predicted that the constant mutation from pre-cancer cells to cancer cells combined with an increased genetic instability may sustain the tumour growth. Numerical simulations with parameter values based on experimental data of breast cancer showed predictions similar to biological observations. The necessary time for tumour progression and diagnosis was estimated for several parameters values, and may range from 2 to 80 years, being very sensible to the apoptotic rate of cancer cells, the mutation rate of premalignant cells and the initial number of mutant cells.

Our model did not consider spacial heterogeneity, which is very important to almost all types of cancer, since all cell interactions and signalling take place in the tumour microenvironment. However, even by adopting a simplified description of such reality, our model provided functional and mechanistic insights to the understanding of cancer as a multi-step process. As a further step, spacial heterogeneity could be considered by an extended model, which should also include other hallmarks of cancer, such as angiogenesis and acid-mediated invasion (Gatenby & Gawlinski, 2003; Hanahan & Weinberg, 2011), two phenomena where spatial configuration plays a major role.

Acknowledgements

The authors are very grateful to the reviewers, whose suggestions improved the quality of the paper.

References

Abbott, R. G., Forrest, S. & Pienta, K. J. (2006) Simulating the hallmarks of cancer. *Artif. Life*, **12**, 617–634.

Ashkenazi, R., Gentry, S. N. & Jackson, T. L. (2008) Pathways to tumorigenesis-modeling mutation acquisition in stem cells and their progeny. *Neoplasia*, **10**, 1170–IN6.

Bellomo, N. & Delitala, M. (2008) From the mathematical kinetic, and stochastic game theory to modelling mutations, onset, progression and immune competition of cancer cells. *Phys. Life Rev.*, **5**, 183–206.

Danial, N. N. & Korsmeyer, S. J. (2004) Cell death: critical control points. *Cell*, **116**, 205–219.

d'Onofrio, A. & Tomlinson, I. P. (2007) A nonlinear mathematical model of cell turnover, differentiation and tumorigenesis in the intestinal crypt. *J. Theor. Biol.*, **244**, 367–374.

Enderling, H., Chaplain, M. A., Anderson, A. R. & Vaidya, J. S. (2007) A mathematical model of breast cancer development, local treatment and recurrence. *J. Theor. Biol.*, **246**, 245–259.

Fassoni, A. C. & Yang, H. M. (2016) An ecological resilience perspective on cancer: insights from a toy model. *Ecol. Complexity*, **30**, 34–46.

Finn, O. J. (2008) Cancer immunology. *N. Engl. J. Med.*, **358**, 2704–2715.

Foulds, L. (1954) The experimental study of tumor progression: a review. *Cancer Res.*, **14**, 327–339.

Fumia, H. F. & Martins, M. L. (2013) Boolean network model for cancer pathways: predicting carcinogenesis and targeted therapy outcomes. *PLoS One*, **8**, e69008.

Gatenby, R. A. & Gawlinski, E. T. (2003) The glycolytic phenotype in carcinogenesis and tumor invasion insights through mathematical models. *Cancer Res*., **63**, 3847–3854.

Gentry, S. N. & Jackson, T. L. (2013) A mathematical model of cancer stem cell driven tumor initiation: implications of niche size and loss of homeostatic regulatory mechanisms. *PLoS One*, **8**, e71128.

Hanahan, D. & Weinberg, R. A. (2000) The hallmarks of cancer. *Cell*, **100**, 57–70.

Hanahan, D. & Weinberg, R. A. (2011) Hallmarks of cancer: the next generation. *Cell*, **144**, 646–674.

Jackson, A. L. & Loeb, L. A. (1998) The mutation rate and cancer. *Genetics*, **148**, 1483–1490.

Loeb, L. A. (1991) Mutator phenotype may be required for multistage carcinogenesis. *Cancer Res*., **51**.

Marciniak-Czochra, A. & Kimmel, M. (2008) Reaction-difusion model of early carcinogenesis: the effects of influx of mutated cells. *Math. Model. Nat. Phenomena*, **3**, 90–114.

Negrini, S., Gorgoulis, V. G. & Halazonetis, T. D. (2010) Genomic instability—an evolving hallmark of cancer. *Nat. Rev. Mol. Cell Biol.*, **11**, 220–228.

Nowell, P. C. (1976) The clonal evolution of tumor cell populations. *Science*, **194**, 23–28.

Ruggiero, R. A. & Bustuoabad, O. D. (2006) The biological sense of cancer: a hypothesis. *Theor. Biol. Med. Model*., **3**, 43.

Salk, J. J., Fox, E. J. & Loeb, L. A. (2010) Mutational heterogeneity in human cancers: origin and consequences. *Annu. Rev. Pathol. Mech. Dis.*, **5**, 51–75.

Schabel, F. M. (1975) Concepts for systemic treatment of micrometastases. *Cancer*, **35**, 15–24.

Spencer, S. L., Berryman, M. J., Garcia, J. A. & Abbott, D. (2004) An ordinary differential equation model for the multistep transformation to cancer. *J. Theor. Biol.*, **231**, 515–524.

Spencer, S. L., Gerety, R. A., Pienta, K. J. & Forrest, S. (2006) Modeling somatic evolution in tumorigenesis. *PLoS Comput. Biol.*, **2**, e108.

Stiehl, T. & Marciniak-Czochra, A. (2012) Mathematical modeling of leukemogenesis and cancer stem cell dynamics. *Math. Model. Nat. Phenomena*, **7**, 166–202.

Tomlinson, I. P. & Bodmer, W. F. (1995) Failure of programmed cell death and differentiation as causes of tumors: some simple mathematical models. *Proc. Natl. Acad. Sci.*, **92**, 11130–11134.

Tomlinson, I. P., Novelli, M. R. & Bodmer, W. F. (1996) The mutation rate and cancer. *Proc. Natl. Acad. Sci.*, **93**, 14800–14803.

Weinberg, R. (2013) *The Biology of Cancer*. New York: Garland Science.

Appendix A. Mathematical analysis of nontrivial equilibria

In this Appendix, we present the proofs and details concerning the existence and stability of internal equilibria $\tilde{P}_i$, $i = 3, 4, 5, 6$.

A.1 *Existence*

The roots of (3.17) occur at the intersection of the curves of $f(A)$ and $g(A)$ in (3.18). The roots of $f(A)$ are $A = 0, A_M, \bar{A}_1$ and $\bar{A}_2$ (where $\bar{A}_1 < \bar{A}_2$ are the roots of $q(A)$), and their relative positions determine the intervals where $f(A) > 0$. The polynomial $g(A)$ is always positive and has a double root $A = A_m$. If we know the relative positions of roots of f and g, we can determine, through graphical analysis, the position of roots $\tilde{A}_i$, $i = 3, 4, 5, 6$, and then, know which of them give rise to a positive equilibrium $\tilde{P}_i$.

Notice that $\tilde{N} > 0$ whenever $\tilde{A} > 0$. Thus, from the expression of $\tilde{G}$ in (3.16), we obtain the following conditions for an equilibrium point $\tilde{P}_i$ be positive:

1. If $\delta < l_G$ and $\beta_2 < \beta_2^{th}$, then $\tilde{P}_i$ is positive if and only if, the root $\tilde{A}_i$ lies in the interval $I_1 = [0, A_M]$ (which is empty if $\beta_2 < \beta_{2,\delta}^{th}$).
2. If $\delta < l_G$ and $\beta_2 > \beta_2^{th}$, then $\tilde{P}_i$ is positive if and only if, the root $\tilde{A}_i$ lies in the interval $I_2 = [A_m, A_M]$.
3. If $\delta > l_G$ and $\beta_2 < \beta_2^{th}$, then $\tilde{P}_i$ is positive if and only if the root $\tilde{A}_i$ lies in the interval $I_3 = [0, \infty)$.
4. If $\delta > l_G$ and $\beta_2 > \beta_2^{th}$, then $\tilde{P}_i$ is positive if and only if, the root $\tilde{A}_i$ lies in the interval $I_4 = [A_m, \infty)$.

In order to study these conditions, the following thresholds need to be considered:

$$\beta_{2,\delta}^{th,i} = \beta_{2,\delta}^{th} + \frac{(l_G - \delta)\beta_1 \bar{A}_i}{r_N},\ i = 1, 2,\ \delta_1 = \frac{l_G \beta_1 (\bar{A}_2 - \bar{A}_1)}{\mu_N + \beta_1 \bar{A}_2},\ \delta_2 = \frac{l_G \beta_1 \bar{A}_2}{\mu_N + \beta_1 \bar{A}_2}. \tag{A.1}$$

From definitions of β_2^{th}, $\beta_{2,\lambda}^{th,i}, A_m, A_M$ and $\beta_{2,\delta}^{th,i}$, in (3.3), (3.15), (3.19) and (A.1), we obtain the following relations:

$$A_m > 0 \Longleftrightarrow \beta_2 > \beta_2^{th}, \tag{A.2}$$

$$A_M > 0 \Longleftrightarrow \beta_2 > \beta_{2,\delta}^{th} \quad \text{and} \quad \delta < l_G, \tag{A.3}$$

$$\bar{A}_i < A_m \Longleftrightarrow \beta_2 > \beta_{2,\lambda}^{th,i}, \qquad i = 1, 2, \tag{A.4}$$

$$\bar{A}_i < A_M \Longleftrightarrow \beta_2 > \beta_{2,\delta}^{th,i} \quad \text{and} \quad \delta < l_G, \qquad i = 1, 2. \tag{A.5}$$

Further, we have that

$$\begin{gathered} \lim_{A \to \pm\infty} f(A) = -\infty, \quad \text{if} \quad \delta < l_G, \\ \lim_{A \to \pm\infty} f(A) = +\infty, \quad \text{if} \quad \delta > l_G, \text{ and} \\ \lim_{A \to \pm\infty} |f(A)/g(A)| = +\infty. \end{gathered} \tag{A.6}$$

Also, from (A.1), notice that in case II, with $0 < \bar{A}_1 < \bar{A}_2$, we have

$$0 < \delta_1 < \delta_2 < l_G. \tag{A.7}$$

With relations (A.2–A.7), and considering each of the cases I, II and III which determine the existence of positive roots $\bar{A}_1$ and $\bar{A}_2$ for $q(A)$ in (3.6), we have all information about the roots of $f(A)$ and $g(A)$ and we can determine which root $\tilde{A}_i$, $i = 3, 4, 5, 6$, lies in the appropriate interval I_j. The thresholds for β_2 and δ in each case can be seen in Fig. 1. Some cases below are illustrated in Fig. A1.

A.1.1 *Case I.* Initially we consider $\beta_3 > \beta_3^{th}$ and $\beta_1 < \beta_{1,\Delta}^{th}$. In this case, the roots $\bar{A}_i$, $i = 1, 2$, are complex or negative. a–c) For $\delta < l_G$, the thresholds for β_2 which are of interest are $0 < \beta_{2,\delta}^{th} < \beta_2^{th}$. We have the following.

a) If $\beta_2 < \beta_{2,\delta}^{th}$, the feasibility interval I_1 is empty. Thus, there is no positive equilibrium $\tilde{P}_i$.

b) If $\beta_{2,\delta}^{th} < \beta_2 < \beta_2^{th}$, then, from (A.2) and (A.3), we have $A_m < 0 < A_M$. The curves of $f(A)$ and $g(A)$ may intersect zero or twice in the interval I_1. It depends on the value of ξ. For ξ below a certain threshold ξ^{th}, the graphic of $g(A)$ intersects the curve of $f(A)$ twice. For $\xi > \xi^{th}$, the curves do not intersect. The value of ξ^{th} is the value of ξ such that the curves of f and g are tangent at a root $\tilde{A}$. Thus, $(\xi^{th}, \tilde{A})$ is a solution to the system

$$\begin{cases} f(A) = g(A) \\ f'(A) = g'(A) \end{cases}. \tag{A.8}$$

Thus, two equilibria, say $\tilde{P}_5$ and $\tilde{P}_6$, are both positive, or all equilibria are non-positive.

c) If $\beta_2 > \beta_2^{th}$, we have $0 < A_m < A_M$. The curves of f and g intersect at $\tilde{A}_5 < A_m$ and at $\tilde{A}_6 \in I_2$. Therefore, $\tilde{P}_6$ is the unique positive equilibrium $\tilde{P}_i$.

d–e) For $\delta > l_G$, the thresholds for β_2 satisfy $\beta_{2,\delta}^{th} < 0 < \beta_2^{th}$. We have the following:

d) If $\beta_2 < \beta_2^{th}$, then $A_M < A_m < 0$. As $f(A)$ is a fourth-degree polynomial, while $g(A)$ has degree two, from (A.6) we have that $f(A) > g(A)$ for A sufficiently large. As $f(0) = 0 < g(0)$, there is at least one root $\tilde{A}_i$ in the interval $I_3 = [0, \infty)$. Other two roots can both lie in this interval, depending on other parameters, such as above. Therefore, equilibrium $\tilde{P}_4$ is positive, and $\tilde{P}_5$ and $\tilde{P}_6$ may be both positive.

e) If $\beta_2 > \beta_2^{th}$, then $A_M < 0 < A_m$. The curves of f and g intersect at one root in the interval $(0, A_m)$, but it does not result in a positive $\tilde{P}_i$. It is possible that the curves intersect twice or zero in the interval (A_m, ∞). Thus, no point $\tilde{P}_i$ is positive, or $\tilde{P}_5$ and $\tilde{P}_6$ are both positive.

A.1.2 *Case II.* Now, we consider $\beta_3 > \beta_3^{th}$ and $\beta_1 > \beta_{1,\Delta}^{th}$. In this case, the roots $\bar{A}_1$ and $\bar{A}_2$ are positive, with $\bar{A}_1 < \bar{A}_2$.

a–h) For $\delta < l_G$, we have the following:

a) If $\beta_2 < \beta_{2,\delta}^{th}$, there is no positive $\tilde{P}_i$, since I_1 is empty.

b) If $\beta_{2,\delta}^{th} < \beta_2 < \min\{\beta_2^{th}, \beta_{2,\delta}^{th,2}\}$, we have $A_m < 0 < \min\{\bar{A}_1, A_M\} < \max\{\bar{A}_1, A_M\} < \bar{A}_2$. Thus, $f(A)$ is positive only in the interval I_2 for values $A \in [0, \min\{\bar{A}_1, A_M\}]$. As $g(A) > 0$ for $A > A_m$, the curves of f and g may intersect zero or twice in I_2, again depending on ξ. Therefore, either there are no positive equilibria $\tilde{P}_i$, or $\tilde{P}_3$ and $\tilde{P}_4$ are positive.

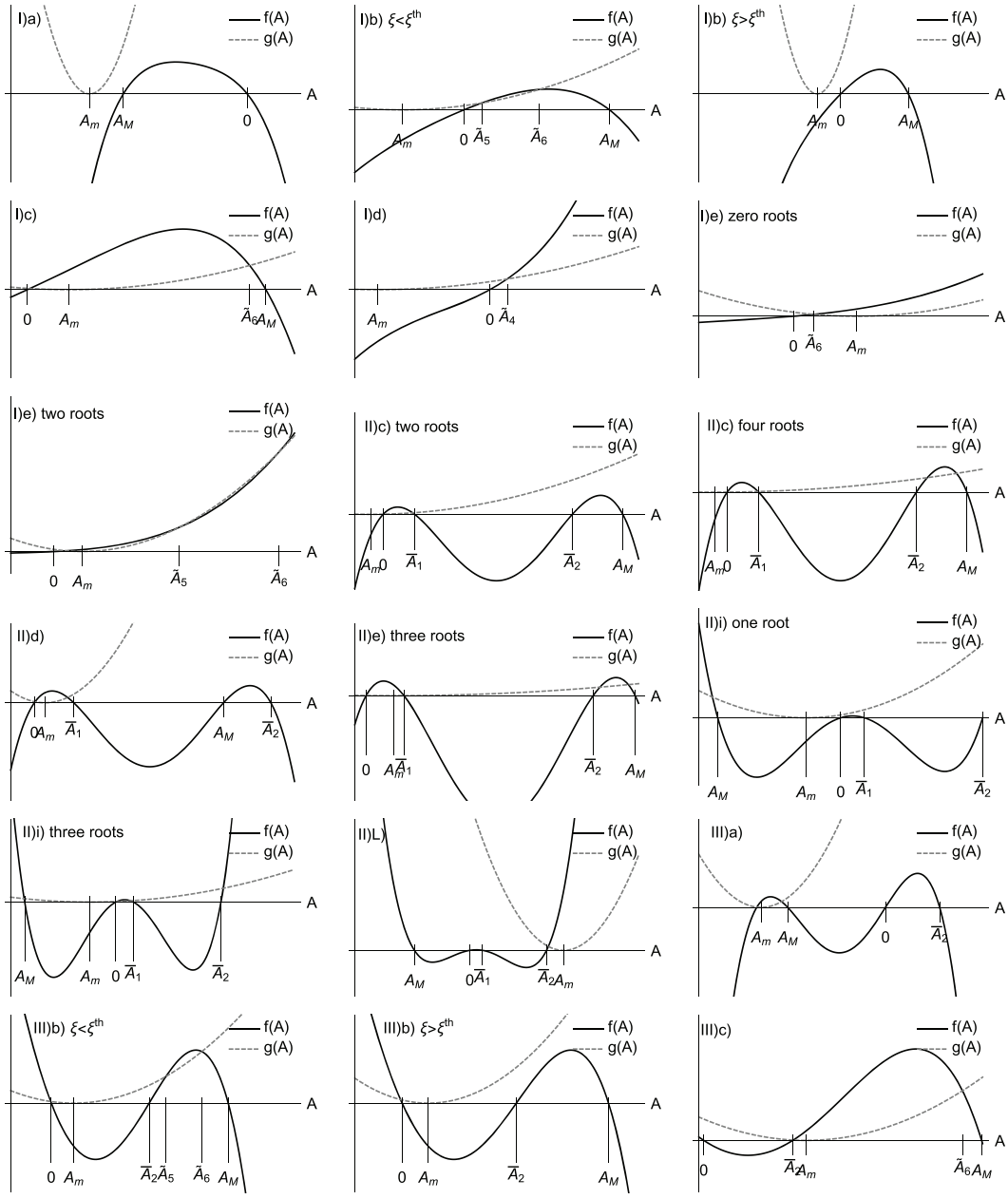

FIG. A1. Curves of $f(A)$ and $g(A)$ in various subcases. The roots of equation (3.17) are the intersecting points of both curves, and must occur at an appropriated interval I_j, in order to give origin to positive equilibria $\tilde{P}_i$. The roots of $f(A)$ are $A = 0, A_M, \bar{A}_1, \bar{A}_2$ and their positions determine the intervals where $f(A) > 0$. The polynomial $g(A)$ is always positive and has a double root $A = A_m$.

c) If $\beta_{2,\delta}^{th,2} < \beta_2 < \beta_2^{th}$, then $A_m < 0 < \bar{A}_1 < \bar{A}_2 < A_M$. The curves of f and g may intersect zero or twice in the interval $[0, \bar{A}_1]$, and also zero or twice in the interval $[\bar{A}_2, A_M]$. Thus, equilibria $\tilde{P}_3$ and $\tilde{P}_4$ may be both positive or not, and the same happens with $\tilde{P}_5$ and $\tilde{P}_6$. Therefore, we may have zero, two or four positive equilibria $\tilde{P}_i$.

d) If $\beta_2^{th} < \beta_2 < \min\{\beta_{2,\lambda}^{th,1}, \beta_{2,\delta}^{th,2}\}$, then $0 < A_m < \min\{\bar{A}_1, A_M\} < \max\{\bar{A}_1, A_M\} < \bar{A}_2$. Thus, since $f(A)$ is positive in the interval I_2 only if $A \in [A_m, \min\{\bar{A}_1, A_M\}]$, and since $g(A_m) = 0$, the unique root in the interval I_2 is $\tilde{A}_4$. Therefore, $\tilde{P}_4$ is the unique positive nontrivial equilibrium.

e) If $\max\{\beta_2^{th}, \beta_{2,\delta}^{th,2}\} < \beta_2 < \beta_{2,\lambda}^{th,1}$, then $0 < A_m < \bar{A}_1 < \bar{A}_2 < A_M$. We have $f(A) > 0$ for $A \in (A_m, \bar{A}_1) \cup (\bar{A}_2, A_M)$. As $g(A_m) = 0$, the unique root in $(A_m, \bar{A}_1)$ is $\tilde{A}_4$. The roots $\tilde{A}_5$ and $\tilde{A}_6$ may both lie in $(\bar{A}_2, A_M)$, or both do not exist, depending on the value of ξ. Therefore, $\tilde{P}_4$ is positive and $\tilde{P}_5$ and $\tilde{P}_6$ may be both positive or not.

f) If $\beta_{2,\lambda}^{th,1} < \beta_2 < \beta_{2,\delta}^{th,2}$, then $0 < \bar{A}_1 < A_m < A_M < \bar{A}_2$. Therefore, $f(A) < 0$ in I_2, in such way no $\tilde{P}_i$ is positive, $i = 3, 4, 5, 6$.

g) If $\max\{\beta_{2,\delta}^{th,2}, \beta_{2,\lambda}^{th,1}\} < \beta_2 < \beta_{2,\lambda}^{th,2}$, then $0 < \bar{A}_1 < A_m < \bar{A}_2 < A_M$. At I_2, we have $f(A) > 0$ only if $A \in [\bar{A}_2, A_M]$. Thus, the curves of f and g can intersect zero or twice (at $\tilde{A}_5$ and $\tilde{A}_6$) in the interval I_2. Therefore, only $\tilde{P}_5$ and $\tilde{P}_6$ may be positive.

h) If $\beta_2 > \beta_{2,\lambda}^{th,2}$, then $0 < \bar{A}_1 < \bar{A}_2 < A_m < A_M$. The curves of f and g intersect exactly once in I_2, at $\tilde{A}_6$. Only $\tilde{P}_6$ is positive.

i–l) For $\delta > l_G$, we have the following.

i) If $\beta_2 < \beta_2^{th}$, then $\min\{A_m, A_M\} < \max\{A_m, A_M\} < 0 < \bar{A}_1 < \bar{A}_2$. At the interval I_3, f is positive when $0 < A < \bar{A}_1$ or $A > \bar{A}_2$. As $g(A_m) = 0$, from (A.6), there is a root $\tilde{A}_6 > \bar{A}_2$. At the interval $0 < A < \bar{A}_1$, the curves can intersect zero or twice (at $\tilde{A}_4$ and $\tilde{A}_5$). Therefore, $\tilde{P}_6$ is positive and $\tilde{P}_4$ and $\tilde{P}_5$ may be positive.

j) If $\beta_2^{th} < \beta_2 < \beta_{2,\lambda}^{th,1}$, then $A_M < 0 < A_m < \bar{A}_1 < \bar{A}_2$. The curves of f and g intersect twice, at $\tilde{A}_5 < \bar{A}_1$ and $\tilde{A}_6 > \bar{A}_2$. $\tilde{P}_5$ and $\tilde{P}_6$ are positive.

k) If $\beta_{2,\lambda}^{th,1} < \beta_2 < \beta_{2,\lambda}^{th,2}$, we have $A_M < 0 < \bar{A}_1 < A_m < \bar{A}_2$. The curves intersect exactly once in the interval I_4, at $\tilde{A}_6 > \bar{A}_2$. Therefore, only $\tilde{P}_6$ is positive.

l) If $\beta_2 > \beta_{2,\lambda}^{th,2}$, we have $A_M < 0 < \bar{A}_1 < \bar{A}_2 < A_m$. Therefore, the four roots of $f(A)$ occur before A_m, in such way that f is a strictly increasing function for $A > A_m$, because the three possible points where $f'(A) = 0$ lie between the roots of f. As $f(A_m) > 0 = g(A_m)$, the curves cannot intersect in the interval I_4. Therefore, no $\tilde{P}_i$ is positive.

A.1.3 *Case III.* In the third case, when $\beta_3 < \beta_3^{th}$, we have $\bar{A}_1 < 0 < \bar{A}_2$.

a–c) For $\delta < l_G$, we have the following:

a) If $\beta_2 < \beta_{2,\delta}^{th,2}$, there is no positive $\tilde{P}_i$. Indeed, if $\beta_2 < \beta_{2,\delta}^{th,2}$, we have $A_m < A_M < 0 < \bar{A}_2$, and the interval I_1 is empty. If $\beta_{2,\delta}^{th} < \beta_2 < \beta_{2,\delta}^{th,2}$, we have $A_1 < 0 < A_M < \bar{A}_2$, in such way that

$f(A) < 0$ for $A \in [0, A_M]$. As $g(A) \geq 0$, there is no root $\tilde{A}_i$ in the intervals I_1 (for $\beta_2 < \beta_2^{th}$) and I_2 (for $\beta_2 > \beta_2^{th}$).

b) If $\beta_{2,\delta}^{th,2} < \beta_2 < \beta_{2,\lambda}^{th,2}$, then $A_1 < 0 < \bar{A}_2 < A_M$. Thus, $f(A) > 0$ in the interval $[\bar{A}_2, A_M]$. As $A_m < \bar{A}_2$, the curves of $f(A)$ and $g(A)$ may intersect zero or twice in the interval $[\bar{A}_2, A_M] \subset I_j$, $j = 1, 2$. Therefore, there may be zero or two positive equilibria $\tilde{P}_i$, $\tilde{P}_5$ and $\tilde{P}_6$.

c) If $\beta_2 > \beta_{2,\lambda}^{th,2}$, then $\bar{A}_1 < 0 < \bar{A}_2 < A_m < A_M$. Thus, there is exactly one root $\tilde{A}_i$ in the interval I_2. Thus, only $\tilde{P}_6$ is positive.

d–e) If $\delta > l_G$, we have the following:

d) If $\beta_2 < \beta_{2,\lambda}^{th,2}$, then $\min\{\bar{A}_1, A_M\} < \max\{\bar{A}_1, A_M\} < 0 < \bar{A}_2$, with $A_m < \bar{A}_2$. If $A > \max\{A_m, 0\}$, $f(A)$ is positive only if $A > \bar{A}_2$. Thus, there is only one root $\tilde{A}_i > \max\{A_m, 0\}$, which is $\tilde{A}_6$. Therefore, only $\tilde{P}_6$ is positive.

e) If $\beta_2 > \beta_{2,\lambda}^{th,2}$, we have $\min\{\bar{A}_1, A_M\} < \max\{\bar{A}_1, A_M\} < 0 < \bar{A}_2 < A_m$. The curves of f and g can intersect zero or twice (at $\tilde{A}_5, \tilde{A}_6 > A_m$) in the interval I_4. Thus, or $\tilde{P}_5$ and $\tilde{P}_6$ are positive, or no $\tilde{P}_i$ is positive.

A.2 *Linear Stability*

Here we present numerical results concerning the stability of the nontrivial equilibria $\tilde{P}_i$. Conditions (3.22) were studied numerically. By varying β_2, bifurcation diagrams were obtained and stability of each equilibrium $\tilde{P}_i$ was inferred. In each of the cases I, II and III, we fixed δ in a determined region, according to Fig. 1, and allowed β_2 to vary, obtaining the bifurcation diagrams for different intervals of δ. In general, a bifurcation occurs when β_2 surpasses the thresholds that limit the regions a), b), c), etc. The obtained diagrams are presented in Figs A2 and A3. In the main graphic of each figure, the behaviour of roots $\tilde{A}_i$ depending on β_2 is presented, together with the values of A_m and A_M, which delimit the interval where the roots $\tilde{A}_i$ give origin to positive $\tilde{P}_i$ (see Appendix A.1). The values $A_0 = 0$, $\bar{A}_1$ and $\bar{A}_2$, corresponding to equilibria P_0, $\bar{P}_1$ and $\bar{P}_2$, whose existence does not depend on β_2, but stability does, are also plotted in the main graphic. These analyses and figures were done using the software *Mathematica*©. Based on these diagrams, and corroborated by numerical simulations (not shown) and phase portraits like those of Fig. 4, we obtained the conclusions summarized in Figs 2 and 3. We present the reasoning for case I in detail, while we summarize it for cases II and III.

A.2.1 *Case I.* If $\beta_3 > \beta_3^{th}$ and $\beta_1 < \beta_{1,\Delta}^{th}$, P_0 is locally stable, while $\bar{P}_1$ and $\bar{P}_2$ are not positive. Corresponding bifurcation diagrams are presented in Fig. A2.

a–c) For $\delta < l_G$, we have the following:

a) If $\beta_2 < \beta_{2,\delta}^{th}$, there is no positive $\tilde{P}_i$, and P_0 is unstable. Numerical results indicate that all solutions tend to P_∞.

b) If $\beta_{2,\delta}^{th} < \beta_2 < \beta_2^{th}$, P_0 is unstable, and $\tilde{P}_5$ and $\tilde{P}_6$ can be positive, depending on ξ. If it happens, numerical simulations indicate that $\tilde{P}_5$ is stable and $\tilde{P}_6$ is unstable, separating solutions that converge to $\tilde{P}_5$ from those that tend to P_∞.

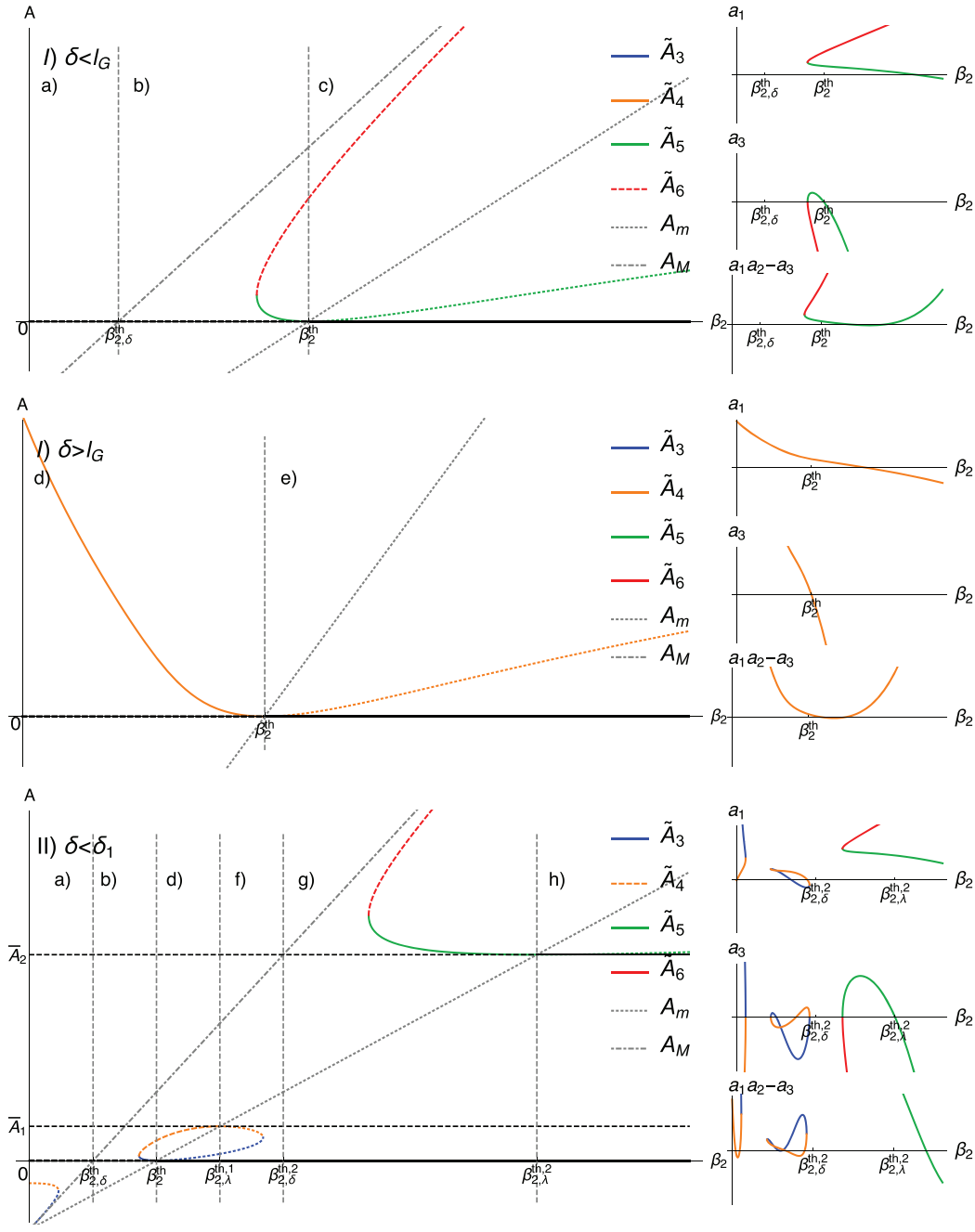

FIG. A2. Bifurcation diagram of equilibria $\tilde{P}_i$ depending on β_2, in cases: I) $\delta < l_G$ (top), I) $\delta > l_G$ (middle) and II) $\delta < \delta_1$ (bottom). Stability of points $\tilde{P}_i$ was determined by observing the curves of coefficients a_1, a_3 e $a_1a_2 - a_3$ (right panels). Plotting is continuous, dashed or dotted, when the corresponding equilibrium is stable, unstable or not positive, respectively.

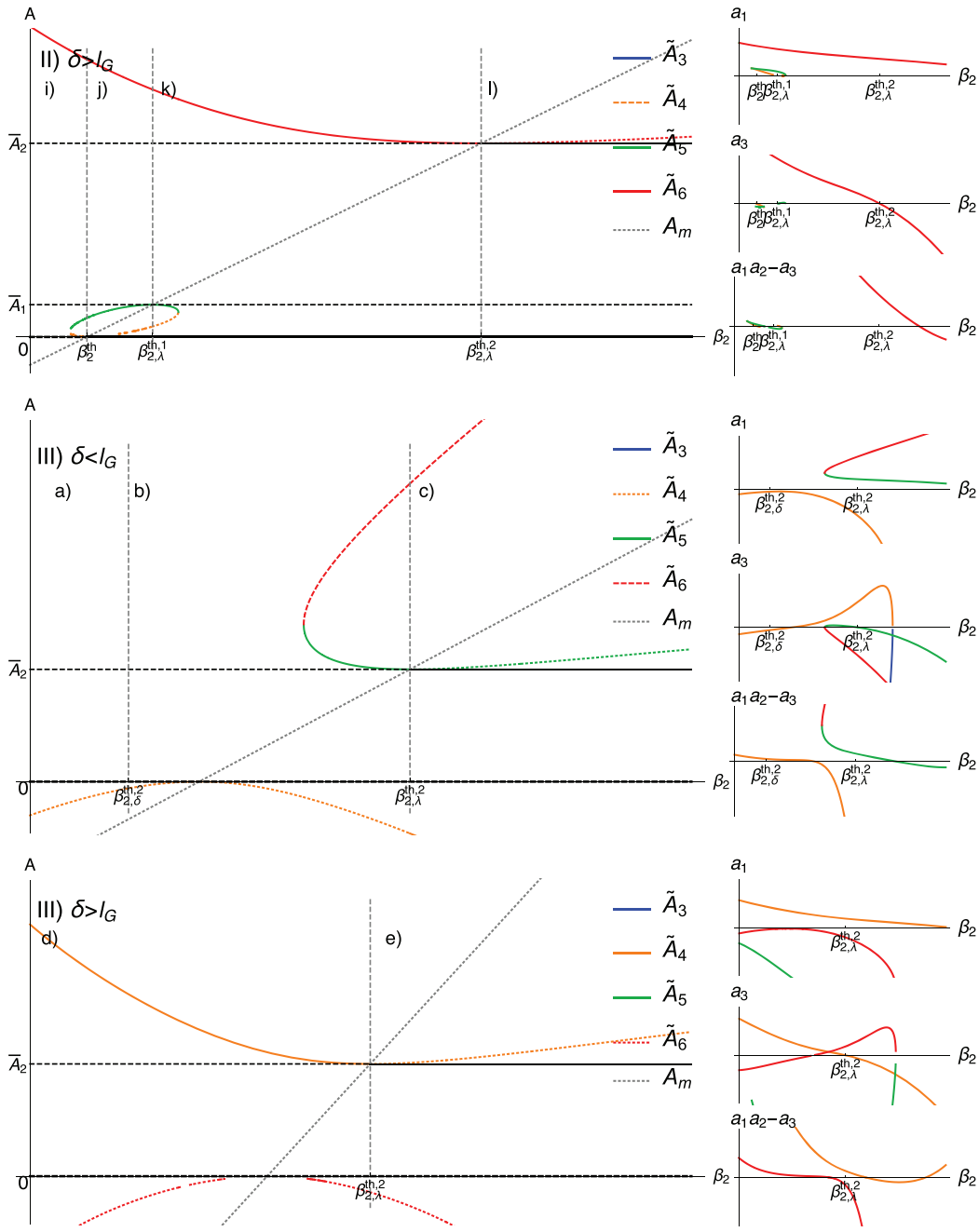

FIG. A3. Bifurcation diagram of equilibria $\tilde{P}_i$ depending on β_2, in cases: II) $\delta > l_G$ (top), III) $\delta < l_G$ (middle) and III) $\delta > l_G$ (bottom). Stability of points $\tilde{P}_i$ was determined by observing the curves of coefficients a_1, a_3 e $a_1a_2 - a_3$ (right panels). Plotting is continuous, dashed or dotted, when the corresponding equilibrium is stable, unstable or not positive, respectively.

c) If $\beta_2 > \beta_2^{th}$, P_0 and $\tilde{P}_6$ are the positive equilibria. P_0 is stable and $\tilde{P}_6$ is unstable, separating the basins of attraction of P_0 and P_∞.

d–e) If $\delta > l_G$, according to the bottom diagram on Fig. A2, we have the following:

d) If $\beta_2 < \beta_2^{th}$, P_0 is unstable. $\tilde{P}_4$ is positive and stable. $\tilde{P}_5$ and $\tilde{P}_6$ can be both positive, depending on ξ. If they are not, numerical simulations indicate that all solutions converge to $\tilde{P}_4$. If $\tilde{P}_5$ and $\tilde{P}_6$ are positive (not shown in Fig. A2), $\tilde{P}_5$ is unstable, separating the basins of attraction of $\tilde{P}_4$ and $\tilde{P}_6$, which are stable.

e) If $\beta_2 > \beta_2^{th}$, $\tilde{P}_4$ is no longer positive and P_0 becomes stable. $\tilde{P}_5$ and $\tilde{P}_6$ can be both positive, and the results are analogous to the previous case.

A.2.2 *Case II.* If $\beta_3 > \beta_3^{th}$ and $\beta_1 > \beta_{1,\Delta}^{th}$, then P_0, $\bar{P}_1$ and $\bar{P}_2$ are positive. $\bar{P}_1$ is unstable. In order to analyse bifurcations with respect to β_2, we must consider four intervals for parameter δ, separated by $0 < \delta_1 < \delta_2 < l_G$. The corresponding bifurcation diagram for the sub-case $0 < \delta < \delta_1$ is presented in Fig. A2. Note that there are no parts c) and e) in this sub-case (see Fig. 1). If $\delta_1 < \delta < \delta_2$, the transitions occur through regions a), b), d), e), g) and h), and for the interval $\delta_2 < \delta < l_G$ the transitions occur through regions a), b), c), e), g) and h). The corresponding bifurcation diagrams for these cases are very similar to the case $0 < \delta < \delta_1$ and are not shown for sake of brevity. For $\delta > l_G$, we have transitions between regions i), j), k) and l), and the bifurcation diagram is shown in Fig. A3.

A.2.3 *Case III.* If $\beta_3 < \beta_3^{th}$, P_0 and $\bar{P}_2$ are positive. P_0 is unstable. The bifurcation diagrams for each of the cases $\delta < l_G$ and $\delta > l_G$ are presented in Fig. A3.